

DTIC FILE COPY

4

ARL-FLIGHT-MECH-TM-417

AR-006-051



DEPARTMENT OF DEFENCE  
DEFENCE SCIENCE AND TECHNOLOGY ORGANISATION  
AERONAUTICAL RESEARCH LABORATORY

MELBOURNE, VICTORIA

AD-A227 749

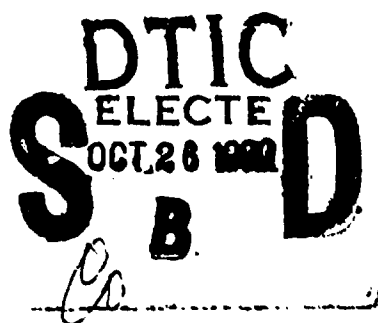
Flight Mechanics Technical Memorandum 417

WIND TUNNEL TESTS OF THE AERODYNAMIC  
CHARACTERISTICS OF A 155 mm ARTILLERY SHELL

by

D.D. SIVAN and C. JERMEY

Best Available Copy

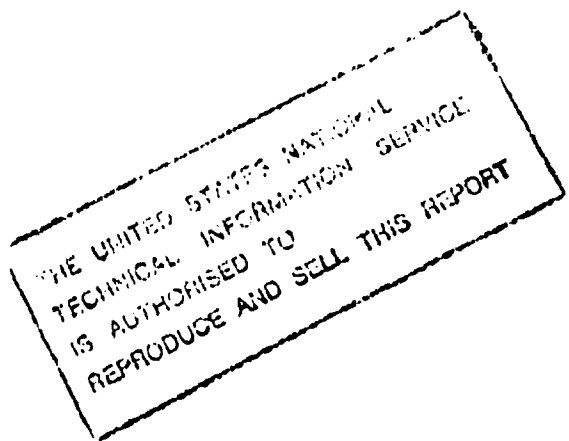


Approved for Public Release.

(C) COMMONWEALTH OF AUSTRALIA 1989

AUGUST 1989

This work is copyright. Apart from any fair dealing for the purpose of study, research, criticism or review, as permitted under the Copyright Act, no part may be reproduced by any process without written permission. Copyright is the responsibility of the Director Publishing and Marketing, AGPS. Inquiries should be directed to the Manager, AGPS Press, Australian Government Publishing Service, GPO Box 84, CANBERRA ACT 2601.



DEPARTMENT OF DEFENCE  
DEFENCE SCIENCE AND TECHNOLOGY ORGANISATION  
AERONAUTICAL RESEARCH LABORATORY

Flight Mechanics Technical Memorandum 417

**WIND TUNNEL TESTS OF THE AERODYNAMIC  
CHARACTERISTICS OF A 155 mm ARTILLERY SHELL**

by

D.D. SIVAN and C. JERMEY

**SUMMARY**

The aerodynamic characteristics of a 1/3rd scale 155 mm artillery shell model were measured as a preliminary step in a program to assess the feasibility of using nose mounted controls on a spinning projectile to control its flight path and hence its point of impact. Tests were conducted for Reynolds numbers of 1.0 to  $4.0 \times 10^5$ , incidences of zero to  $20^\circ$ , Mach numbers of 0.7 to 1.8, and roll rates of zero to 400 rev/s. Results indicate that the use of nose mounted controls to control the attitude and hence the flight path of a 155 mm shell is unlikely to be very effective within the subsonic and transonic Mach number range.



**(C) COMMONWEALTH OF AUSTRALIA 1989**

---

POSTAL ADDRESS: Director, Aeronautical Research Laboratory,  
P.O. Box 4331, Melbourne, Victoria, 3001, Australia

## CONTENTS

	Page
NOTATION	
1. INTRODUCTION .....	1
2. EXPERIMENTAL DETAILS .....	1
2.1 Model and balances .....	1
2.2 Experimental procedure .....	2
2.2.1 Non-spinning tests .....	2
2.2.2 Spinning tests .....	3
2.3 Accuracy of results .....	3
3. PRESENTATION AND DISCUSSION OF RESULTS .....	4
3.1 Presentation of results .....	4
3.2 Test results .....	5
3.2.1 Non-spinning tests .....	5
3.2.2 Spinning tests .....	6
3.3 Concluding remarks .....	7
REFERENCES .....	7

### FIGURES 1 - 12

### DISTRIBUTION LIST

### DOCUMENT CONTROL DATA



Accession For	
NTIS GRAAX <input checked="" type="checkbox"/>	
DTIC TAB <input type="checkbox"/>	
Unannounced <input type="checkbox"/>	
Justification _____	
By _____	
Distribution/ _____	
Availability Codes _____	
Dist	Avail and/or Special
A-1	

### NOTATION

$C(X)$	Axial force coefficient	=	$\frac{X}{qS}$
$C(Y)$	Side force coefficient	=	$\frac{Y}{qS}$
$C(Z)$	Normal force coefficient	=	$\frac{Z}{qS}$
$C(l)$	Rolling moment coefficient	=	$\frac{l}{qSD}$
$C(m)$	Pitching moment coefficient	=	$\frac{m}{qSD}$
$C(n)$	Yawing moment coefficient	=	$\frac{n}{qSD}$
$CP(Z)$	Position of centre of pressure in the pitch plane		
$CP(Y)$	Position of centre of pressure in the yaw plane		
$M$	Mach number of the free stream		
$Re_d$	Reynolds number of free stream, based on maximum body diameter		
$S$	Maximum body cross sectional area, (reference area)		
$D$	Maximum body diameter (reference length)		
$U_\infty$	Velocity of free stream		
$X$	Axial force		
$Y$	Side force		
$Z$	Normal force		
$l$	Rolling moment		
$m$	Pitching moment		
$n$	Yawing moment		
$\omega$	roll rate; clockwise from rear is +ve		
$\omega'$	non-dimensional roll rate	=	$\frac{\omega \pi D}{2U_\infty}$
$q$	dynamic pressure of free stream		
$\Theta$	pitch angle (incidence) relative to free stream		
$\phi$	roll angle		

## 1. INTRODUCTION

This report presents the results of a series of tests on a 1/3 scale model of a 155 mm standard artillery shell conducted in the S-1 Wind Tunnel. These tests were conducted to determine the aerodynamic characteristics of the shell at various spin rates, and over a range of attitudes and Mach numbers. This work was a preliminary step in a program to assess the feasibility of using nose mounted controls on a spinning projectile to control its flight path and hence its point of impact.

The basic equipment for wind tunnel testing of rapidly spinning models already existed as a result of a similar study of a 105 mm artillery shell in late 1977 (see Reference 1 for details) and this equipment required only minor modifications to accommodate the new model. The tests were carried out during August and September of 1987. This work has been reported earlier in reports prepared for meetings of the TTCP technical panel W-2, and the CAARC Aerodynamics Coordinators (Ref. 2 and 3).

## 2. EXPERIMENTAL DETAILS

### 2.1 Model and balances

Figure 1 shows the basic dimensions of the 1/3rd scale standard 155 mm artillery shell model. All model dimensions were obtained from full scale shell drawings, except for the details of the drive band, which were deduced from an examination of the drawings of the gun barrel rifling grooves. In figure 1 it may be seen that the direction of the rifling grooves on the drive band is opposite to that on the full size shell. This is because the roll drive motor operates only in the opposite sense to the rotation of the full size shell. Consequently, all spin rates, Magnus forces and Magnus moments were of opposite sign to those existing on the full size shell. To avoid confusion, in the presentation of results these signs have been reversed to give data appropriate to the spin direction of the full size shell.

Two different balances were used for non-spinning and spinning tests respectively. Figure 2a shows the model mounted on the non-spinning balance, which is a conventional 6 component strain gauge sting balance, while figure 2b shows the model mounted on the Magnus balance, which is a 4 component balance (measuring  $C(Y)$ ,  $C(Z)$ ,  $C(m)$  &  $C(n)$ ).

Figure 3 shows the internal details of the drive and roll rate measuring system. The model was mounted on the shaft of a sliding-vane type air motor, which incorporated an air-bearing for low friction radial support, and this then fitted to a strain gauge sting balance. High pressure air for the motor was supplied through the hollow core of the balance, and low pressure air for the air-bearing was supplied through two thin tubes taped to the outside of the sting. Model roll rate was monitored by a LED-photodiode roll rate pickup, mounted on the sting and triggered 10 times during each revolution of the model. Roll rate control was effected by varying the air supply pressure to the motor.

Since spin rates of up to 400 rev/s were required, careful dynamic balancing of the model was necessary before wind tunnel tests were commenced. This was accomplished outside the tunnel with the model mounted on the strain gauge balance and the balance outputs monitored on a CRO screen. Observation of the amplitude and phase of the outputs as the model was spun enabled small masses to be determined and positioned on the outside of the model to compensate for the imbalance observed. These balancing masses were then replaced by internal masses and the model spun again as a check. Excellent balance was obtained, with only one fairly "noisy" resonant area at about 35 rev/s, corresponding to resonant oscillation at the natural frequency of the model/balance system. This spin rate was therefore avoided where possible during the wind tunnel tests.

## 2.2 Experimental procedure.

All tests were conducted in the 360 mm x 360 mm working section of the continuous flow wind tunnel S-1 at the Flight Mechanics and Aeropropulsion Division, of ARL-Salisbury. Data for the Mach number range of 0.7 to 1.0 were obtained using slotted top and bottom walls in the working section, while fixed supersonic nozzles were fitted for the supersonic Mach numbers of 1.4 and 1.8.

### 2.2.1 Non-spinning tests

Data were collected for the Reynolds' number range of  $1.0 \times 10^5$  to  $4.0 \times 10^5$  (based on maximum body diameter) at Mach numbers of 0.7, 0.95, 1.4 and 1.8 to assess the sensitivity of the results to variations in Reynolds number. All other tests were conducted at a Reynolds number of  $Re_d = 4.0 \times 10^5$ , this being the nearest possible to flight Reynolds numbers ( $1.0 \times 10^6$  to  $2.0 \times 10^6$ ) without overloading the balance.

The boundary layer trip, described in figure 1, was used to ensure a turbulent boundary layer over the shell body to simulate flow conditions expected at the higher Reynolds numbers of the full scale shell. Surface flow visualization was used to check the effectiveness of the boundary layer trip and it revealed that at low incidences a turbulent boundary layer existed virtually everywhere along the body of the shell, except for a very small portion at the nose tip.

The base pressure on the model was measured and a correction applied such that the  $C(X)$  values presented represent the shell with a uniform pressure, equal to free stream static, acting over the base area. No corrections have been applied to allow for the expected base pressure in flight or for the differences in skin friction coefficient between model and full scale.

The experimental procedure consisted of establishing the required tunnel flow conditions and then conducting pitch and roll traverses for the pitch angle range of  $-4^\circ$  to  $20^\circ$  (in  $1^\circ$  increments) and for the roll angle range of  $0^\circ$  to  $360^\circ$  (in  $15^\circ$  increments). Note that zero roll angle position is defined in figure 4.

### 2.2.2 Spinning tests

Spinning tests were conducted at a fixed Reynolds number of about  $4.0 \times 10^5$  for all Mach numbers. The experimental procedure involved establishing the required tunnel flow conditions, setting the required model roll rate by adjusting the motor supply pressure, and then conducting a pitch traverse of the model from  $-4^\circ$  to  $20^\circ$ , taking data at one degree intervals. For the tests at zero roll rate it was found necessary to shut off the air supply to the model air-bearings, otherwise the torque generated by the grooves of the driving band was sufficient to produce a small steady roll rate. With no air supplied, the friction between the air-bearing surfaces prevented the model from rolling. For consistency, all non-rolling tests were conducted at zero roll orientation, as defined in figure 4.

### 2.3 Accuracy of results

The results consist of aerodynamic force and moment coefficients at given Mach numbers, Reynolds numbers, incidences, roll angles and roll rates. The sources of error and the accuracy applicable to each item are discussed below.

#### (a) Force and moment coefficients

The major sources of error are expected to be due to the dynamic effects of the spinning model (Magnus balance only) i.e., vibration and the discharge of exhaust air. Under static conditions both balances are capable of measuring forces and moments to an accuracy of 0.1%. No attempt was made to calibrate the Magnus balance under dynamic conditions, but comparison of spinning and non-spinning tests indicated that discrepancies were small, generally less than 0.5%. A conservative estimate of the maximum percentage uncertainty in the force and moment coefficients for both balances would therefore be 1%.

An absolute uncertainty also exists in each force and moment coefficient, which is independent of local coefficient value, and arises mainly from the resolution limits of the measuring system, balance drift, temperature changes and noise levels (i.e. vibrations) in the balance output. This uncertainty is variable with Mach number and incidence, but is of a maximum order of 0.01 for all coefficients.

#### (b) Mach numbers

The Mach number is manually controlled from observation of the stagnation pressure in the settling chamber and the static pressure in the working section. Mach numbers are held to within 0.01 of the nominal figure, and this is also the level of spatial uncertainty in the centreline Mach number of the working section. No corrections have been applied for the effects of blockage.

**(c) Reynolds numbers**

The stagnation temperature of the tunnel air flow is uncontrolled and varies slowly during a tunnel run causing a corresponding change in Reynolds number. For each particular run the uncertainty in the Reynolds number was within 5% of the nominal value.

**(d) Pitch and roll angle**

Errors in support attitude measurement and sting bending correction produce an uncertainty in attitude measurement of less than 0.01°. However airflow direction on the tunnel axis is uniform only to within 0.2°, so that this is a more realistic estimate of the uncertainty in the incidences quoted. Roll angles were measured to within 0.1°.

**(e) Roll rate**

Roll rates were obtained from a counter which displayed the total number of pulses received each second from the model, which generated ten pulses per revolution. Data were taken only after a steady roll rate had been reached although small changes inevitably occurred as the incidence was varied during a run. The roll rate given for each data point is therefore accurate to within 0.1 rev/s, but the approximate roll rates for an entire run may have uncertainties of up to 5 revs/s.

### 3. PRESENTATION AND DISCUSSION OF RESULTS

#### 3.1 Presentation of results

Figure 4 shows the axis system used in the presentation of the results. The origin of the system is at the base of the shell model (i.e. 5.630 calibers from the nose tip). The zero roll orientation was chosen to be with the fuse delay adjustment screw hole on the windward streamline.

Results are presented in a coefficient form (using the reference quantities and axis system above) in figures 5 to 11, where selected results have been plotted to illustrate the trends revealed as functions of incidence, Mach number, Reynolds number, roll angle and roll rate.

### 3.2 Test results

#### 3.2.1 Non-spinning tests

##### (a) Effect of roll angle

The effect of roll angle was found to be negligible for all but the  $C(Y)$  and  $C(n)$  coefficients at incidences greater than  $15^\circ$ . Figure 5 illustrates the variation of the measured coefficients with roll angle at a Mach number of 0.7 and  $20^\circ$  incidence. The variation shown in the  $C(Y)$  and  $C(n)$  coefficients is most probably attributable to asymmetric vortex separation of the cross flow due to slight asymmetries of the model.

##### (b) Effect of Reynolds number

Figure 6 shows the effect of Reynolds number on  $C(X)$ ,  $C(Z)$  and  $C(m)$  coefficients. The effect of Reynolds number on all other coefficients was very small. The variation of  $C(X)$  with Reynolds number, at low incidence, is consistent with expected changes in skin friction coefficient, while changes occurring in  $C(Z)$  and  $C(m)$  at high incidence are due to changes in cross flow drag coefficient with Reynolds number. The changes in cross flow drag coefficient, which are produced by changes in flow separation in the cross-flow plane of the body, reduce the Reynolds number dependence of  $C(X)$  at the higher incidences. The observed changes in  $C(Z)$  and  $C(m)$  at high incidence indicate that the cross flow characteristics of the shell are above the critical at the highest Reynolds number and therefore the results would be expected to be in close agreement with full scale.

##### (c) Effect of Mach number and incidence

Values of the side force and yawing moment coefficients are near zero below  $15^\circ$  incidence (for all Mach numbers) but increase noticeably thereafter indicating the beginning of an asymmetric vortex wake. No side force and yawing moment data are presented here; they are covered later under the effects of spin rate. The rolling moment coefficient,  $C(l)$ , is near zero throughout the pitch and Mach number range and therefore no data is presented.

The wind tunnel  $C(X)$  data, at the maximum test Reynolds number, and for a base pressure coefficient of zero, is compared with flight measured data (reference 6) in figure 7.

Figure 8 shows the effect of Mach number and incidence on  $C(X)$ ,  $C(Z)$ ,  $C(m)$  and  $CP(Z)$  coefficients. The normal force and pitching moment coefficients are continuous functions of incidence up to  $20^\circ$  for all Mach numbers. Note that the pitching moment data is calculated relative to the base of the shell rather than its centre of gravity and so may be less meaningful than the centre of pressure in the pitch plane, which is plotted in figure 8d. This shows that for subsonic

conditions the centre of pressure is well forward throughout the incidence range, generally less than 2 calibres from the nose, and varies considerably with Mach number and incidence, being furthest forward for transonic and low incidence conditions. The supersonic centres of pressure within the incidence range are further back (up to  $2\frac{1}{2}$  calibres from the nose) and are less variable with incidence. Note that the centres of pressure have been derived from the division of a moment coefficient by a force coefficient for incidences above 4°, and have been faired into a zero incidence value determined by the ratio of the slopes of the same coefficients against incidence.

### 3.2.2 Spinning tests

#### (a) Comparison of results from spinning and non-spinning balances

As detailed in Section 2.1, the spinning tests were conducted on a separate balance which measured  $C(Y)$ ,  $C(Z)$ ,  $C(m)$  and  $C(n)$  only. Prior to the spinning tests, non-rolling results were obtained for the maximum Reynolds number case with the model static in the zero roll orientation. These results were compared to non-spinning balance data and the correlation was found to be excellent for all coefficients throughout the full incidence and Mach number range. The correlation between  $C(Z)$  and  $C(m)$  data for Mach number = 1.0 is illustrated in figure 9.

No base pressure or internal pressures were measured for the spinning tests and any effect of turbine and bearing air exhaust on the measured coefficients is not known but is believed to be small.

#### (b) Effect of spin rate

Figure 10 illustrates that spin rate was found to have little effect on the normal force and pitching moment coefficients, but a significant effect on side force and yawing moment. Therefore no  $C(Z)$  or  $C(m)$  data are presented here, since they have been previously covered under non-spinning tests.

Figure 11 shows the effects of incidence and spin rate on the side (Magnus) force and yawing moment coefficients. The side force and yawing moment coefficients increase linearly with increasing spin rate and incidence at the lower Mach numbers. However the rate of increase reduces as the Mach number increases and the results become more nonlinear, particularly at transonic and low supersonic speeds.

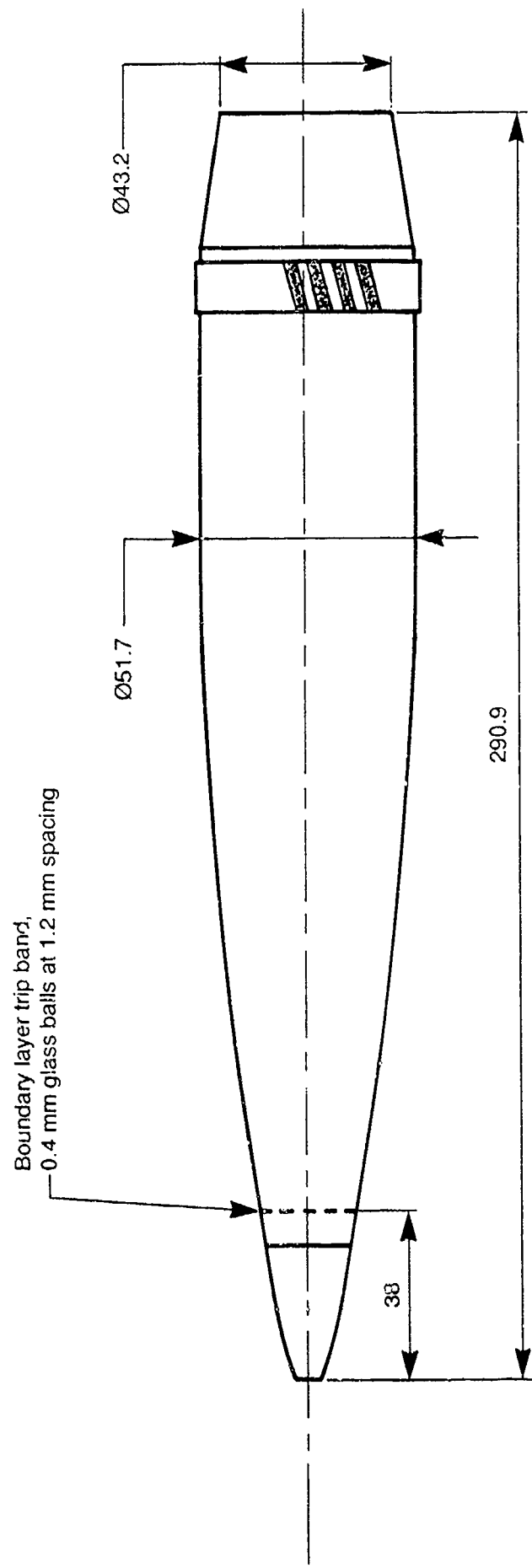
Figure 12 shows a plot of the centre of pressure of the side (Magnus) force vs Mach number at the maximum spin rate tested. It was found that in general the position of CP(Y) was not very sensitive to the magnitude of the spin rate and the trends shown here are typical for all other spin rates. The anomalous point at an incidence of 15° and a Mach number of 1.4 is produced by the discontinuities in the slopes of the C(Y) and C(n) curves against spin rate for this condition as shown in figures 11(k) and 11(l). The relative magnitudes of these slope changes indicate that the loss of side force (below a possible linear increase with spin rate) is occurring in the boattail region of the shell. It is known that the reflected bow shock waves pass close to the shell base for this Mach number but it is not known if this is the source of the anomaly or if it is due to an interaction between the cross flow separation and the shell spin rate.

### 3.3 Concluding remarks

The results indicate that the use of nose-mounted controls to control the attitude and hence the flight path of a 155mm shell is unlikely to be very effective within the subsonic and transonic Mach number range. This is because the centre of pressure in the pitch plane is situated very close to the likely control position, and is strongly affected by Mach number and incidence. A control force applied near the nose to produce trim at incidence would therefore be almost equal and opposite to the body normal force. The resultant normal force coefficient at trim (zero pitching moment) would be small and highly variable with Mach number and incidence. This is particularly true at low incidences. Side (Magnus) forces are also small and are non-linear at high incidences and high Mach numbers, so would also be of limited value for trajectory control.

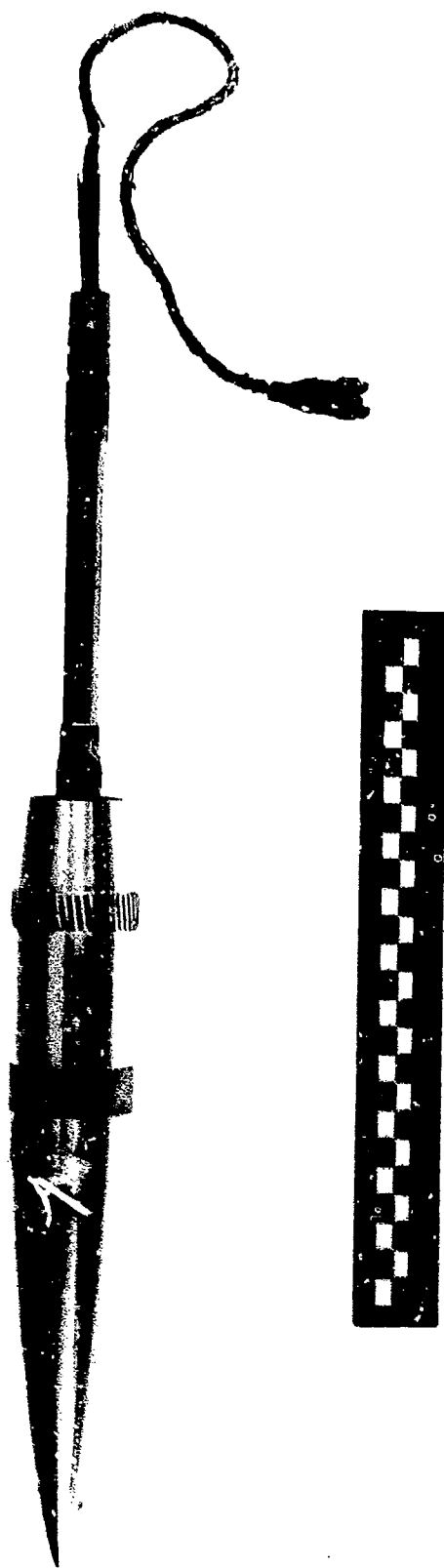
### REFERENCES

NO	AUTHOR	TITLE
1	Jermey, C.	"Wind Tunnel Tests on the Static Aerodynamics of a Spinning 105 mm Artillery Shell Model". WSRL-0020-TR, March 1979
2	Styan, D.D.	"155 mm Artillery Shell-Wind Tunnel Tests". Report prepared for the meeting of TTCP Technical Panel NTP-2, September 1988
3	Styan, D.D.	"155 mm Artillery Shell - Wind Tunnel Tests". Report prepared for the CAARC Aerodynamics Coordinators Meeting, June 1988
4		Unpublished data from RARDE

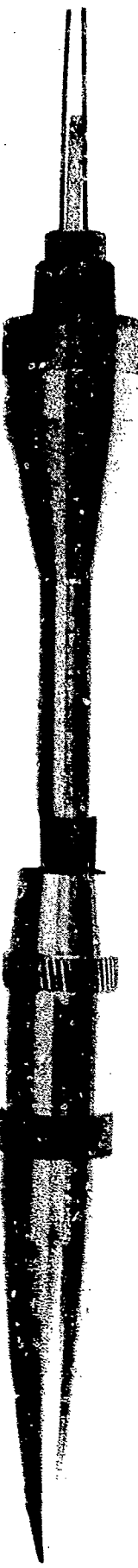


Note: All dimensions in mm

FIGURE 1: 155 mm SHELL - 1/3RD SCALE MODEL DIMENSIONS



(a) Model on the non - spinning balance



(b) Model on the spinning (Magnus) balance

FIGURE 2: ASSEMBLY OF MODEL ON BALANCES

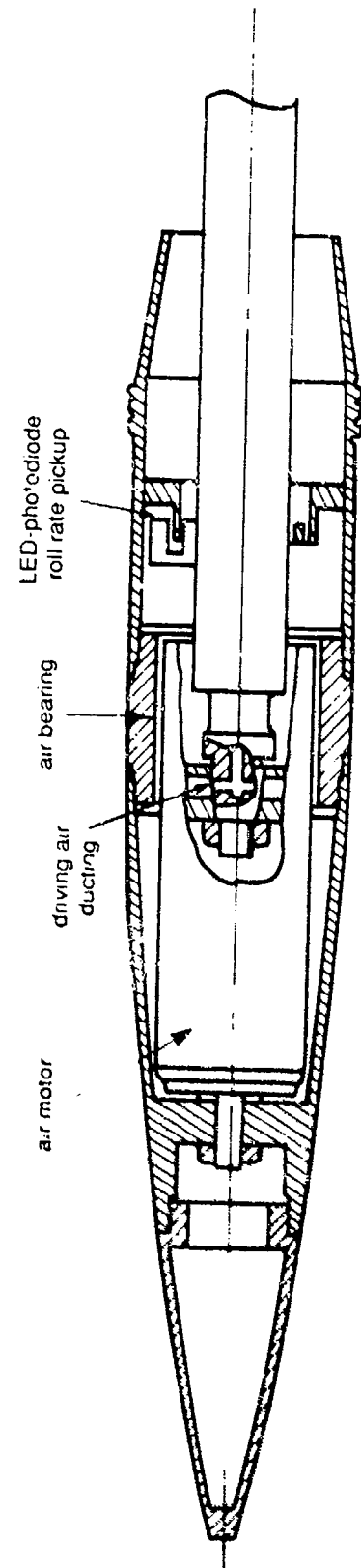


FIGURE 3: MODEL ON THE MAGNUS BALANCE, SHOWING INTERNAL DETAILS

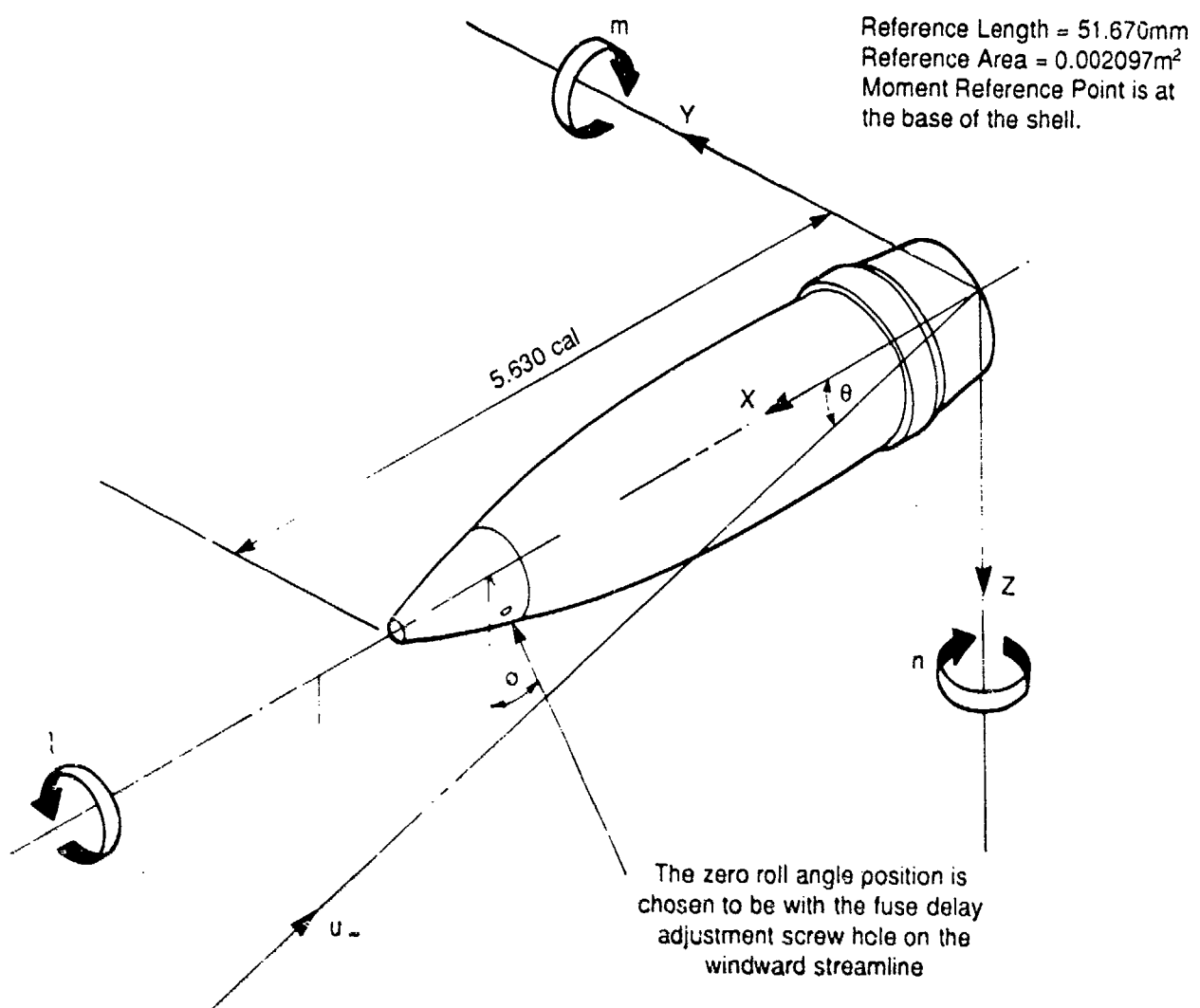
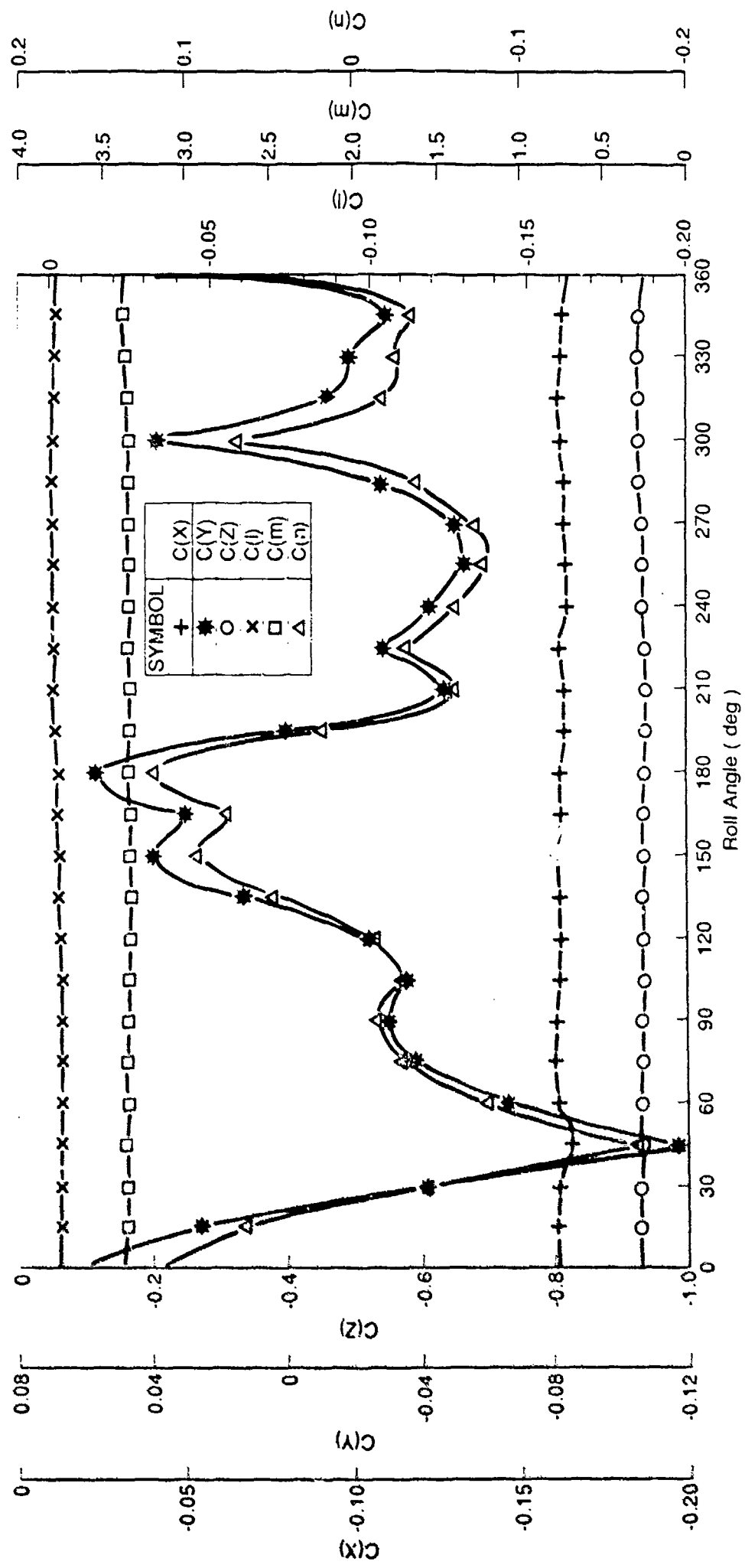
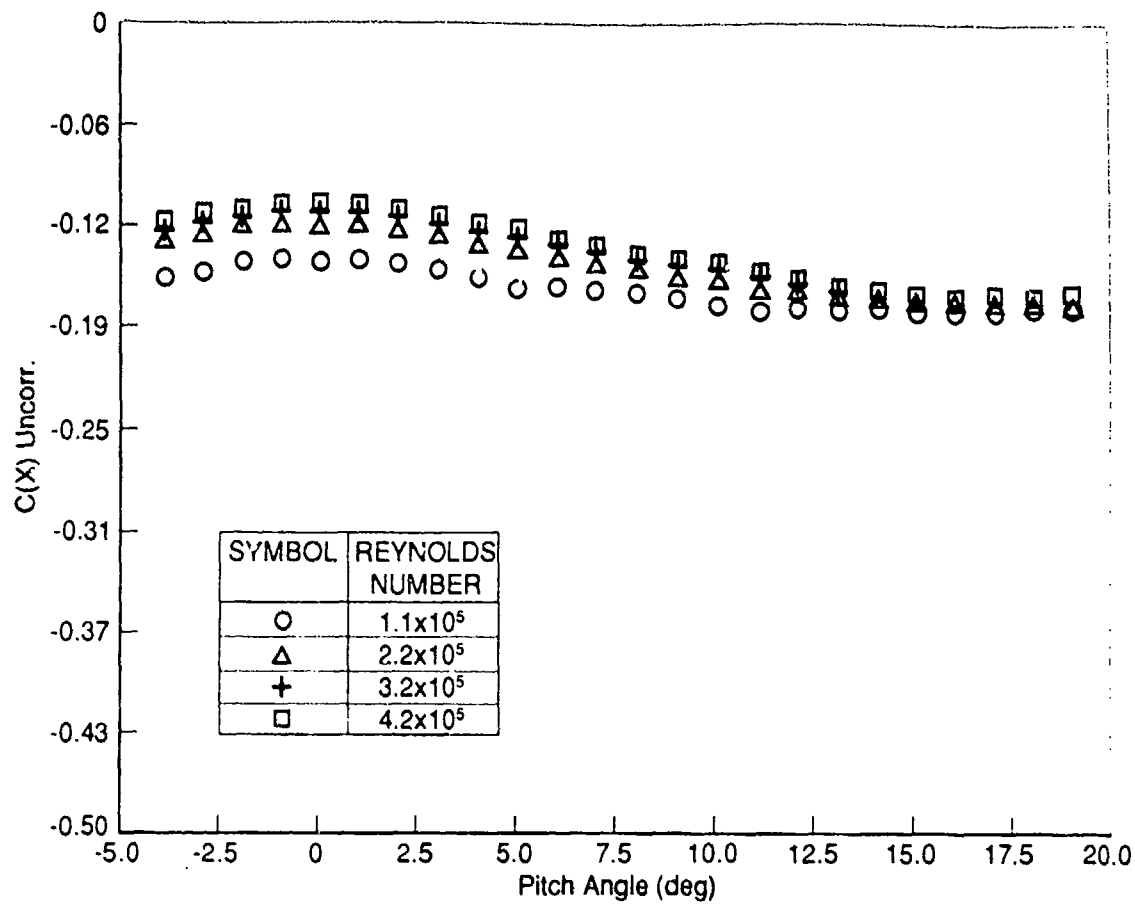
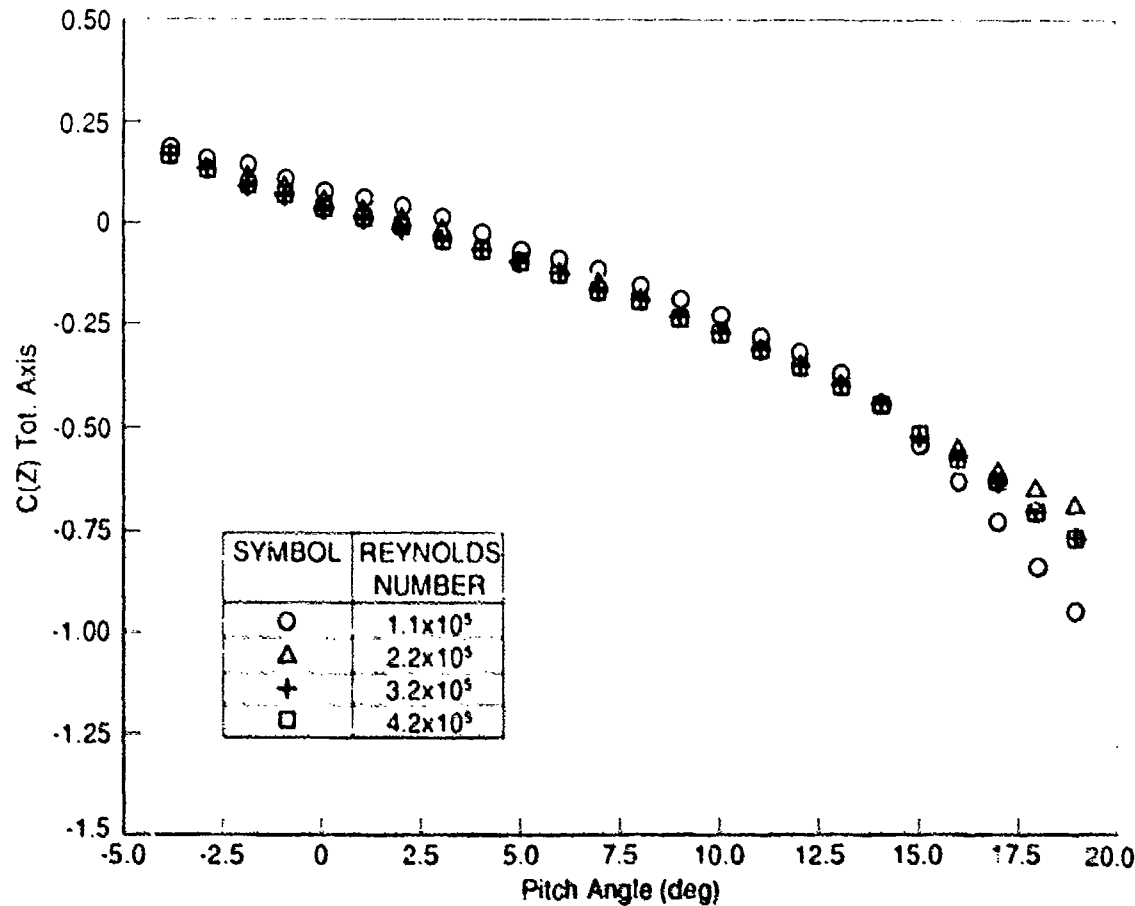


FIGURE 4: AXIS SYSTEM USED IN PRESENTATION OF RESULTS



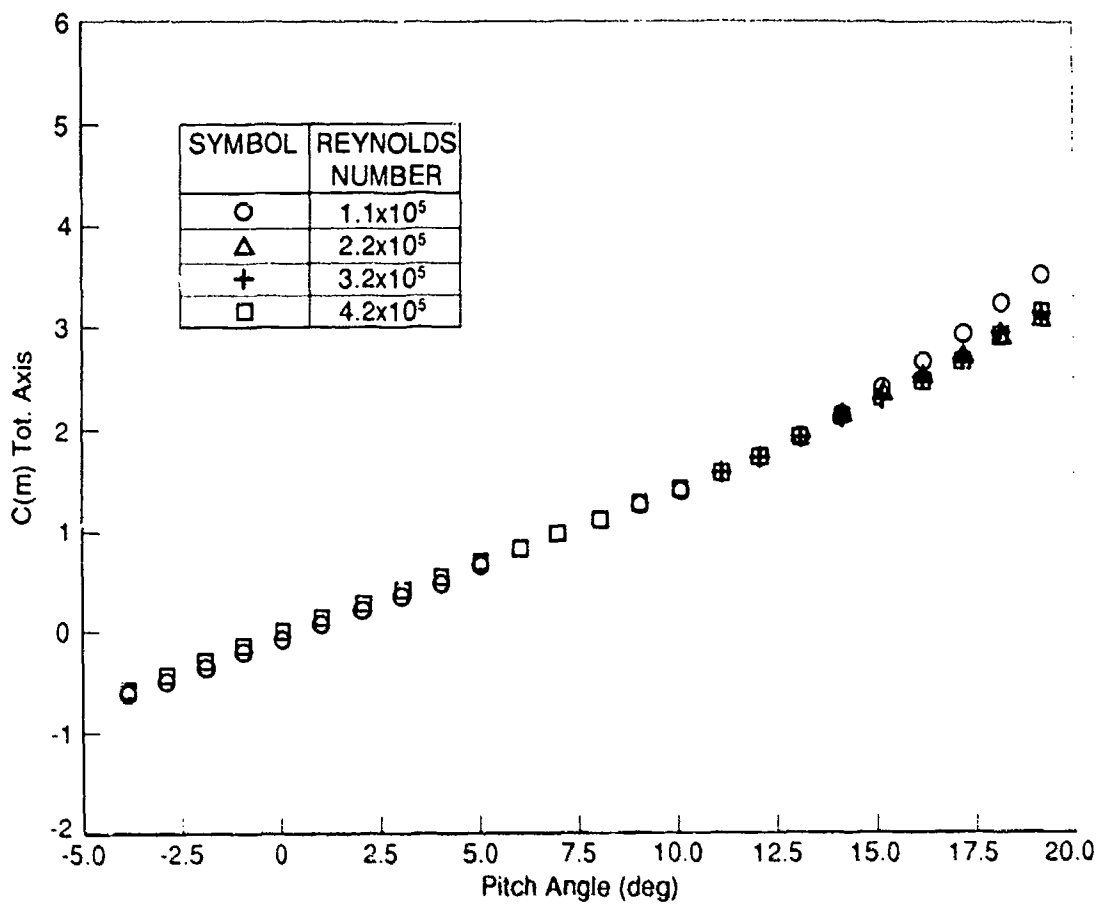


(a) Axial force coefficient,  $C(X)$  vs pitch angle



(b) Normal force coefficient,  $C(Z)$  vs pitch angle

FIGURE 6: EFFECT OF REYNOLDS NUMBER ON AERODYNAMIC COEFFICIENTS  $C(X)$ ,  $C(Z)$  AND  $C(m)$  AT MACH NO. = 0.7 AND ROLL ANGLE = 0°.  
(NON-SPINNING BALANCE)



(c) Pitching moment coefficient,  $C(m)$  vs pitch angle

FIGURE 6: (CONT'D) EFFECT OF REYNOLDS NUMBER ON AERODYNAMIC COEFFICIENTS  $C(X)$ ,  $C(Z)$  AND  $C(m)$  AT MACH NO. = 0.7 AND ROLL ANGLE = 0°. (NON-SPINNING BALANCE)

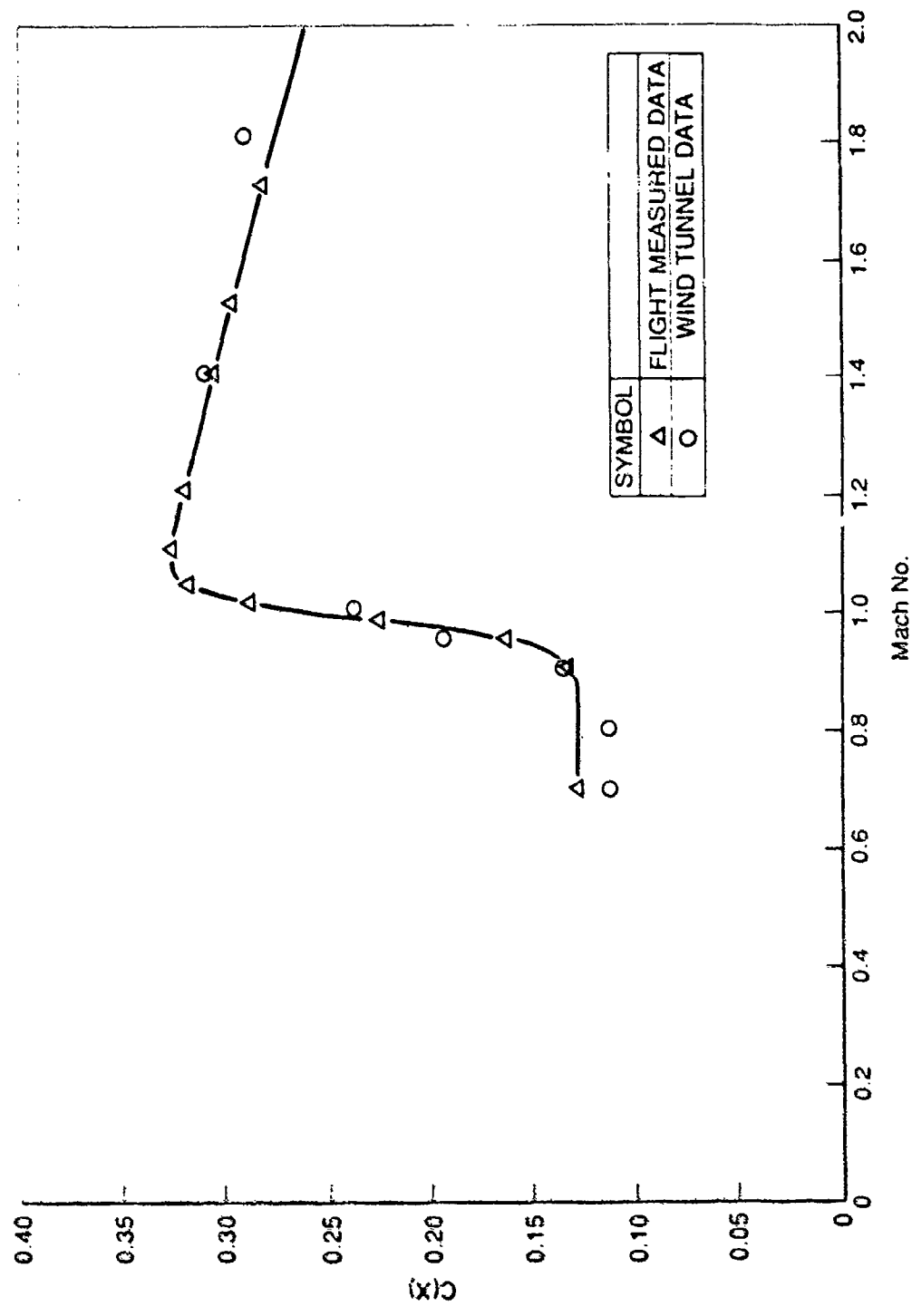
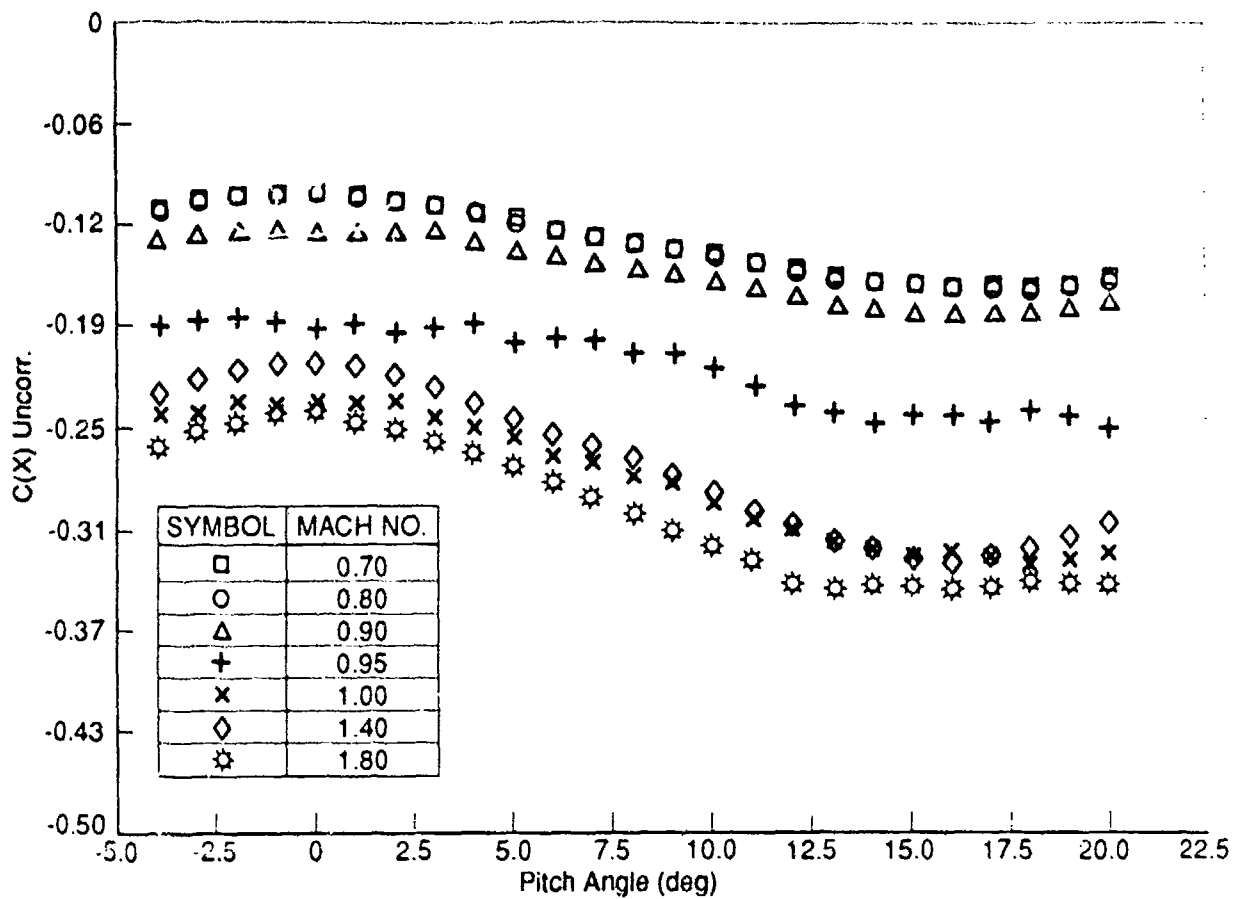
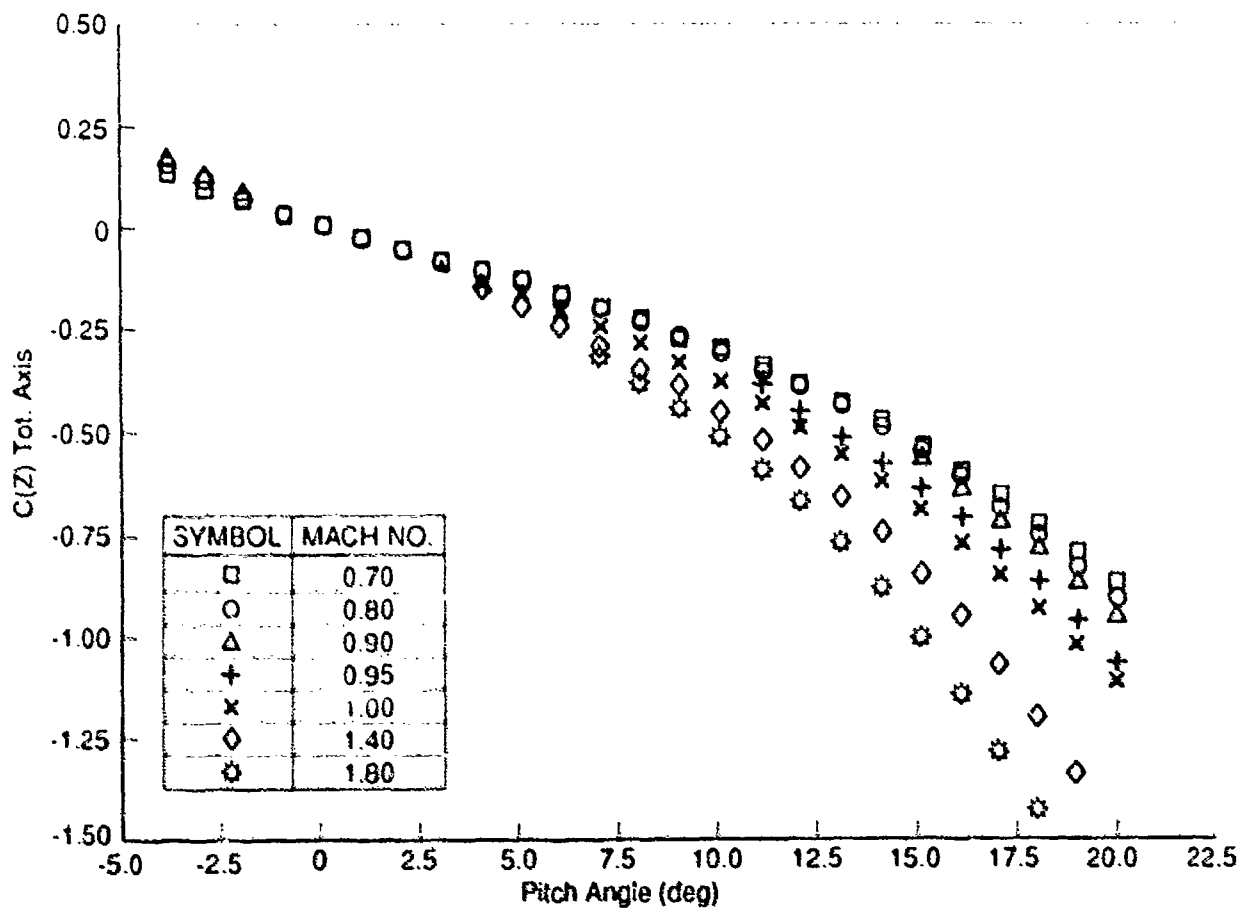


FIGURE 7: COMPARISON OF FLIGHT MEASURED  $C(X)$  DATA WITH WIND TUNNEL RESULTS (NON-SPINNING BALANCE)

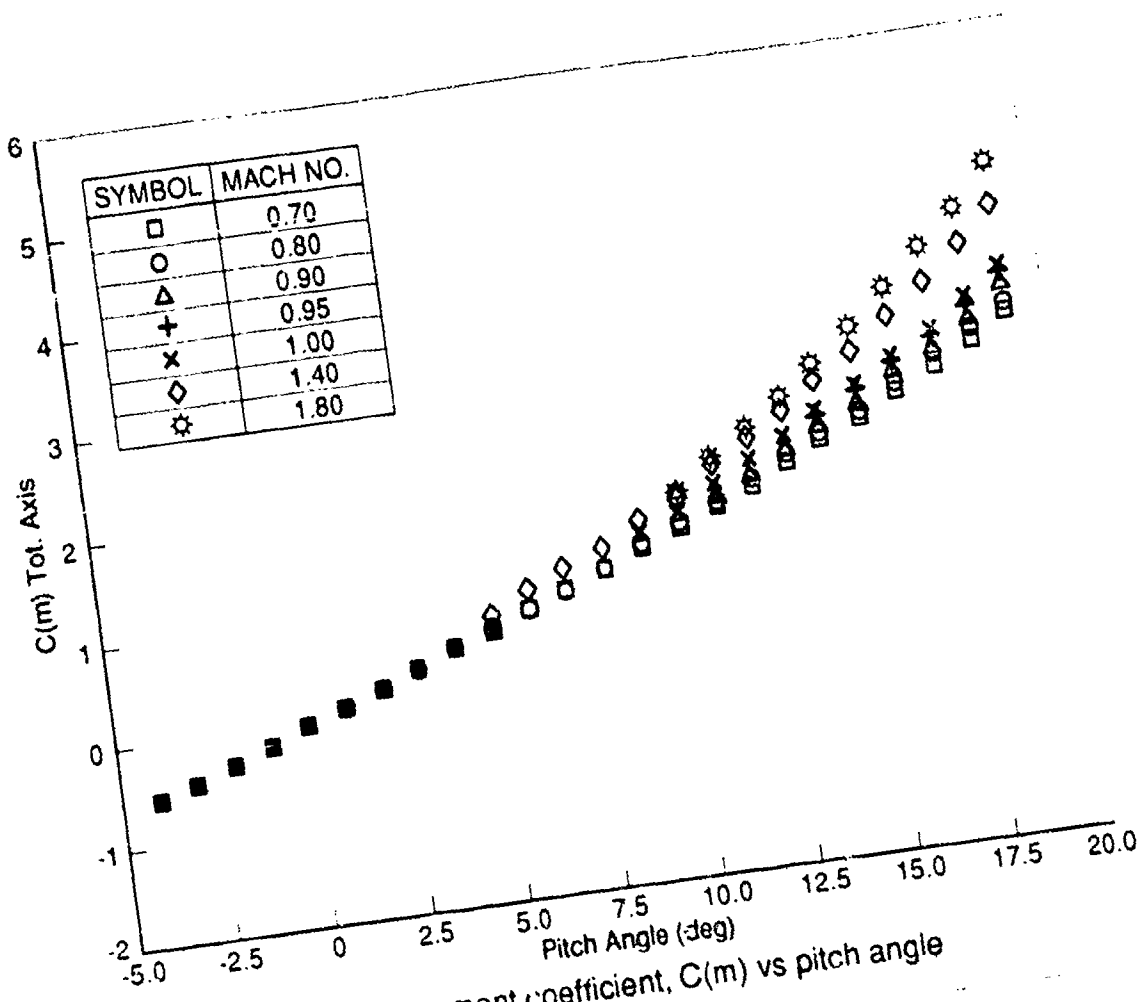


(a) Axial force coefficient,  $C(X)$  vs pitch angle

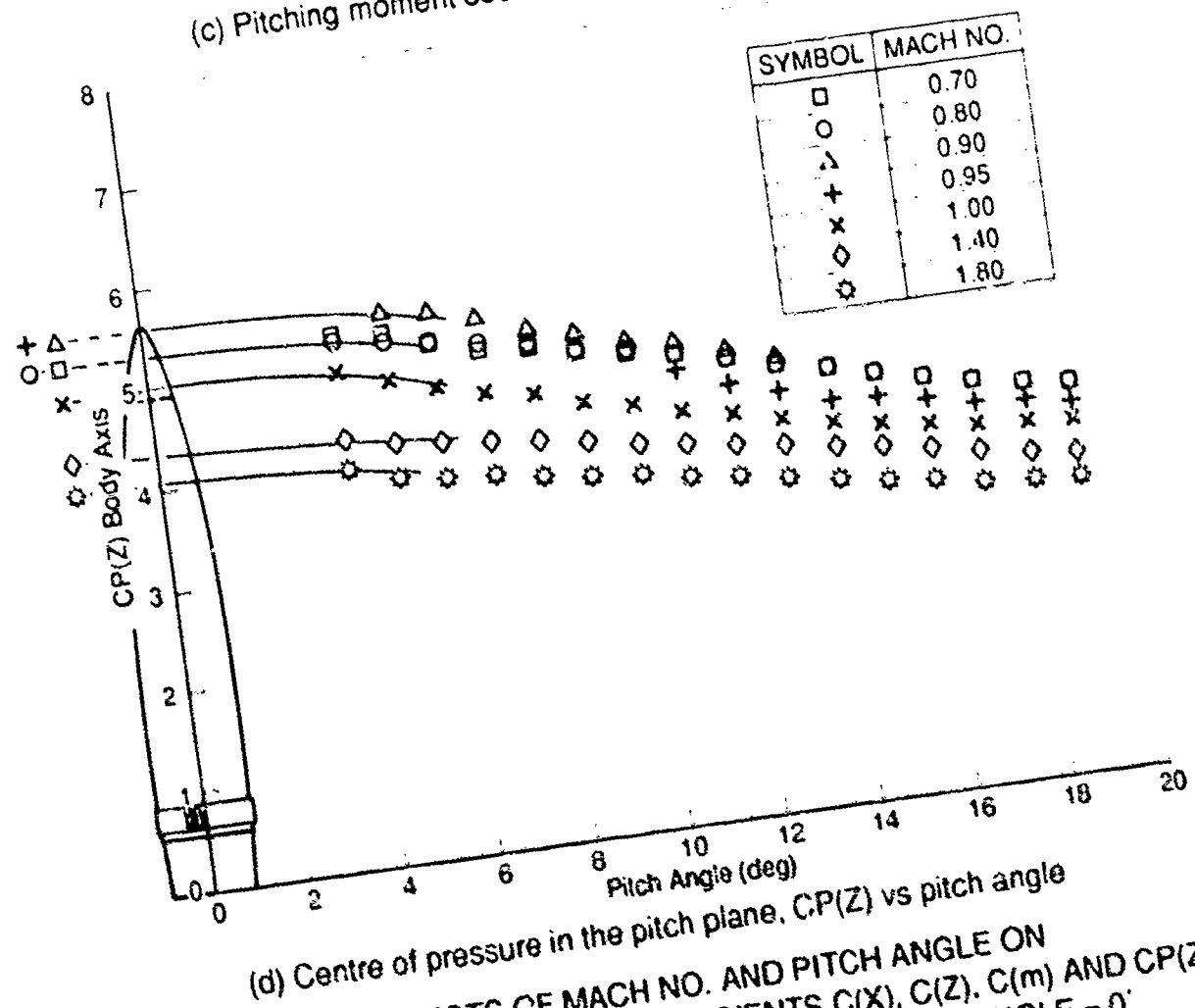


(b) Normal force coefficient,  $C(Z)$  vs pitch angle

FIGURE 8: EFFECTS OF MACH NO. AND PITCH ANGLE ON AERODYNAMIC COEFFICIENTS  $C(X)$ ,  $C(Z)$ ,  $C(m)$  AND  $CP(Z)$  AT REYNOLDS NO. =  $4.0 \times 10^5$  AND AT ROLL ANGLE = 0°. (NON - SPINNING BALANCE).

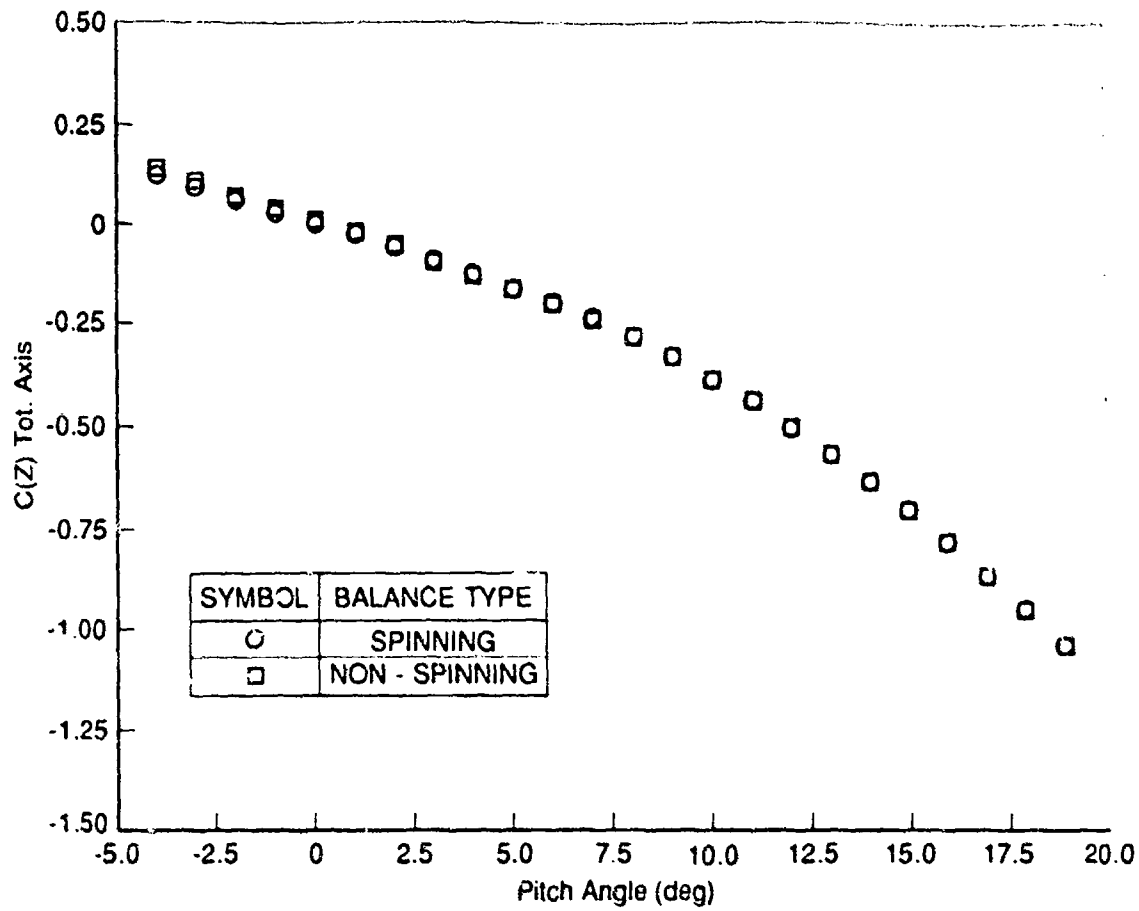


(c) Pitching moment coefficient,  $C(m)$  vs pitch angle

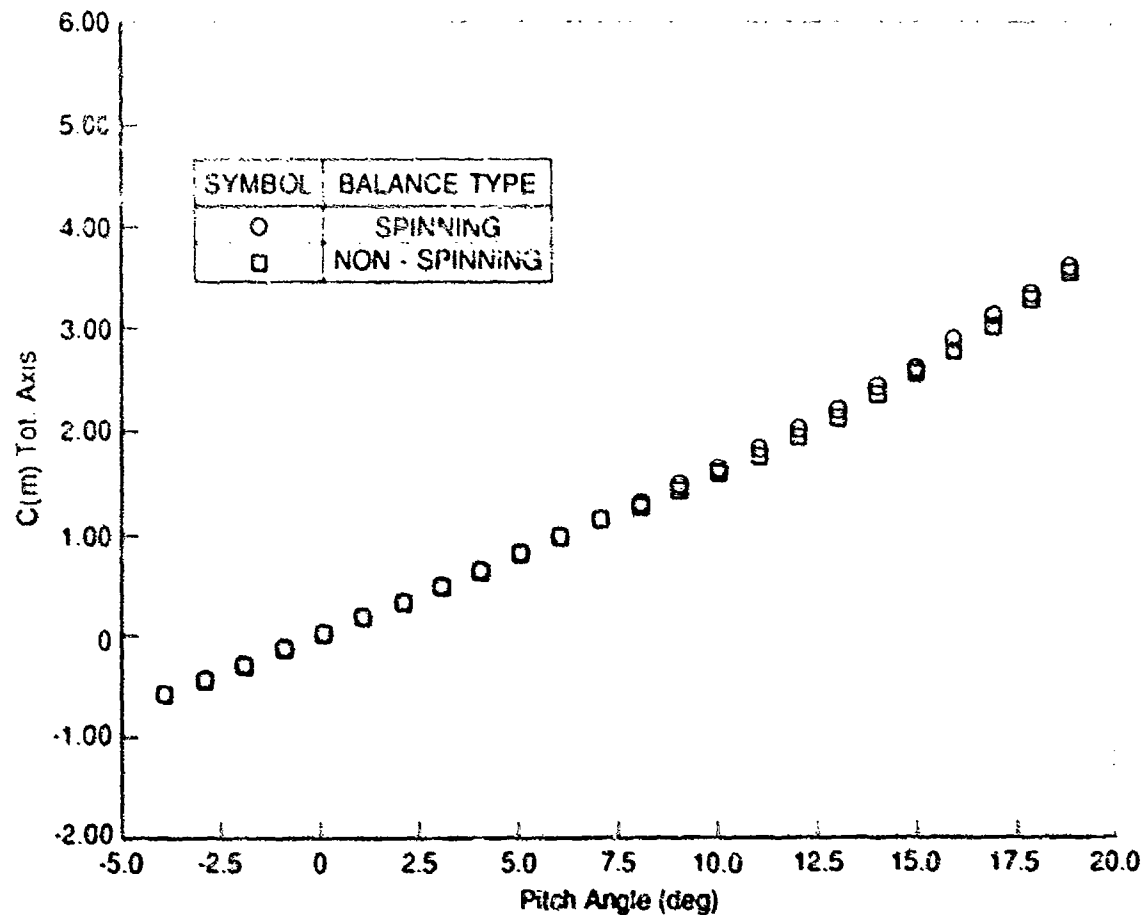


(d) Centre of pressure in the pitch plane,  $CP(Z)$  vs pitch angle

FIGURE 8: (CONT'D) EFFECTS OF MACH NO. AND PITCH ANGLE ON AERODYNAMIC COEFFICIENTS  $C(X)$ ,  $C(Z)$ ,  $C(m)$  AND  $CP(Z)$  AT REYNOLDS NO. =  $4.0 \times 10^5$  AND AT ROLL ANGLE =  $0^\circ$ .  
(NON-SPINNING BALANCE).



(a)  $C(Z)$  coefficient (static conditions, zero Roll angle) at Mach No. = 1.0



(b)  $C(m)$  coefficient (static conditions, zero Roll angle) at Mach No. = 1.0

FIGURE 9: COMPARISON OF STATIC RESULTS FROM SPINNING AND NON-SPINNING BALANCES.

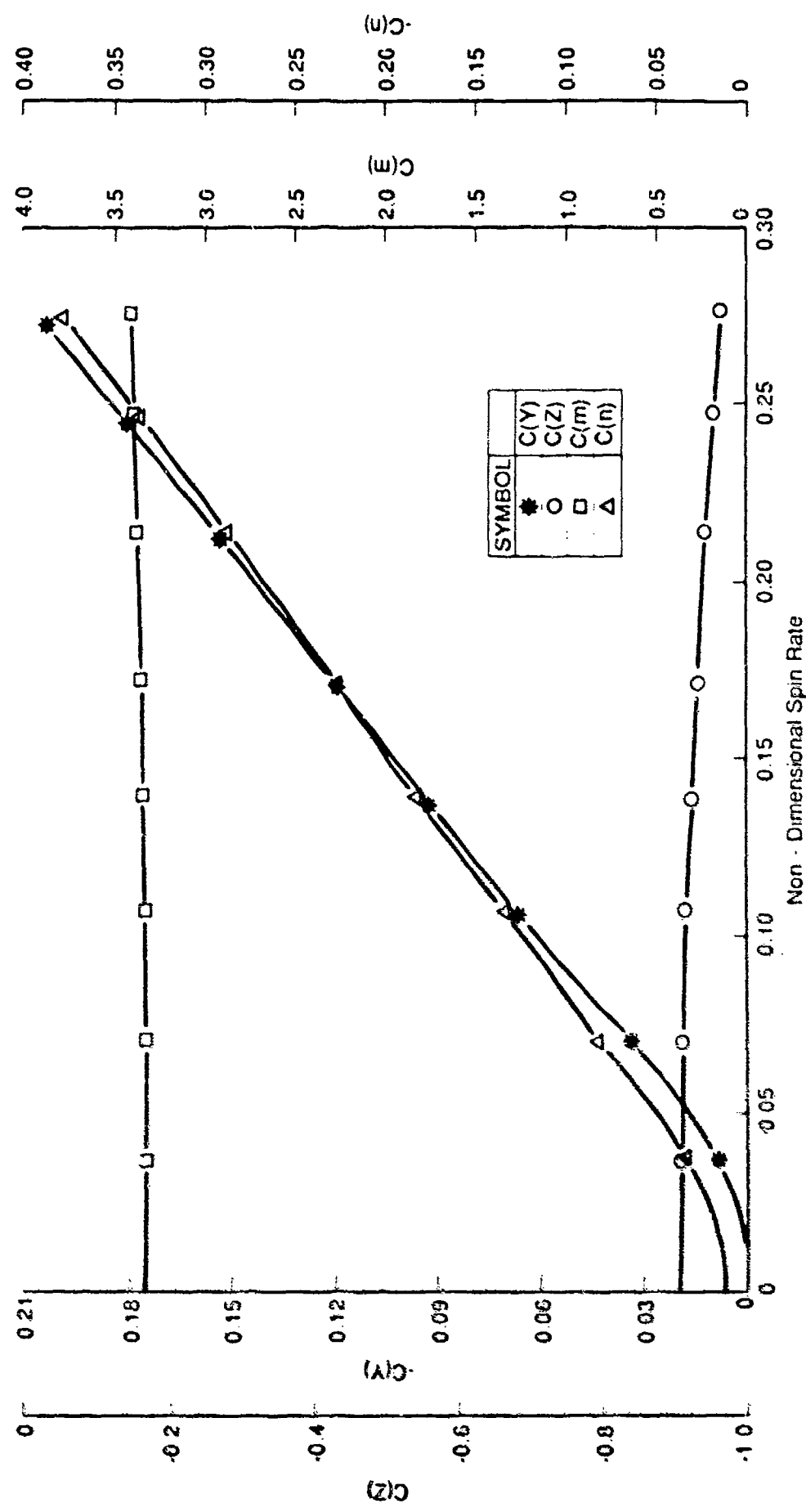
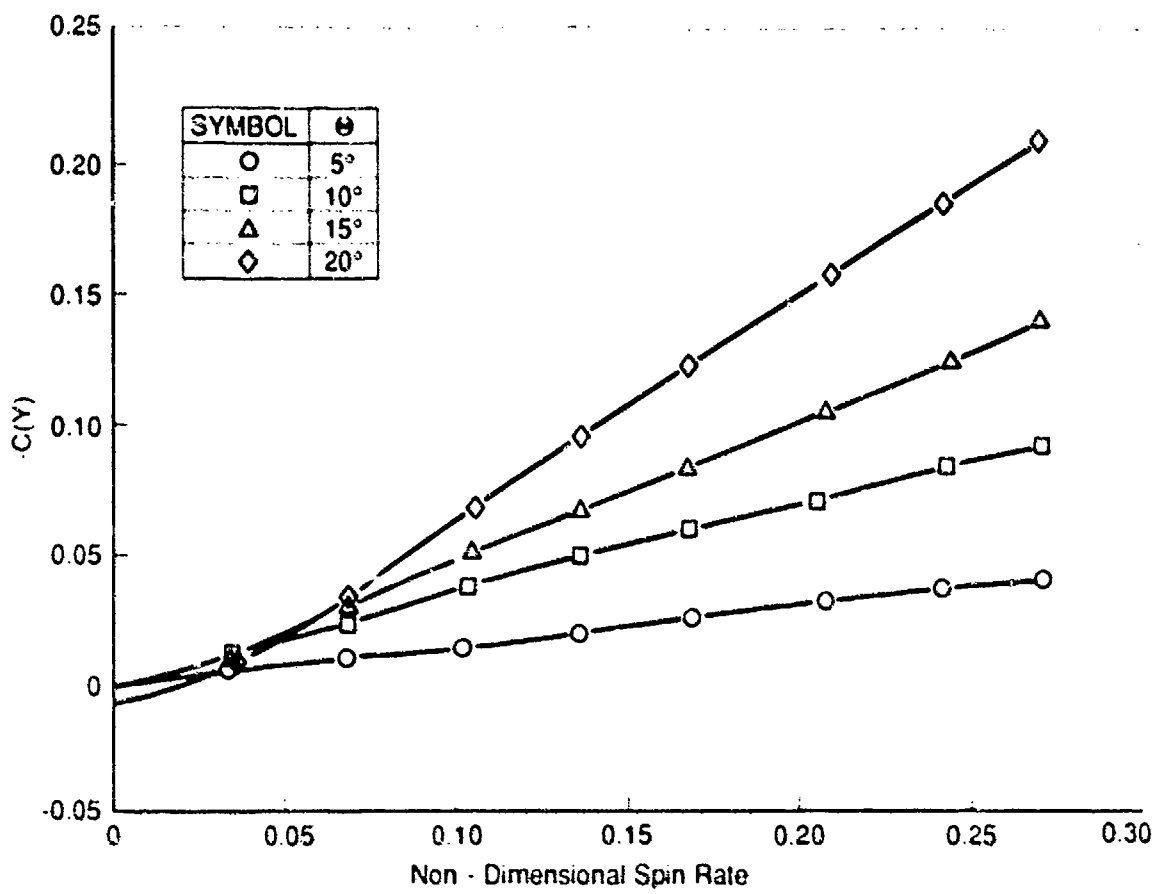
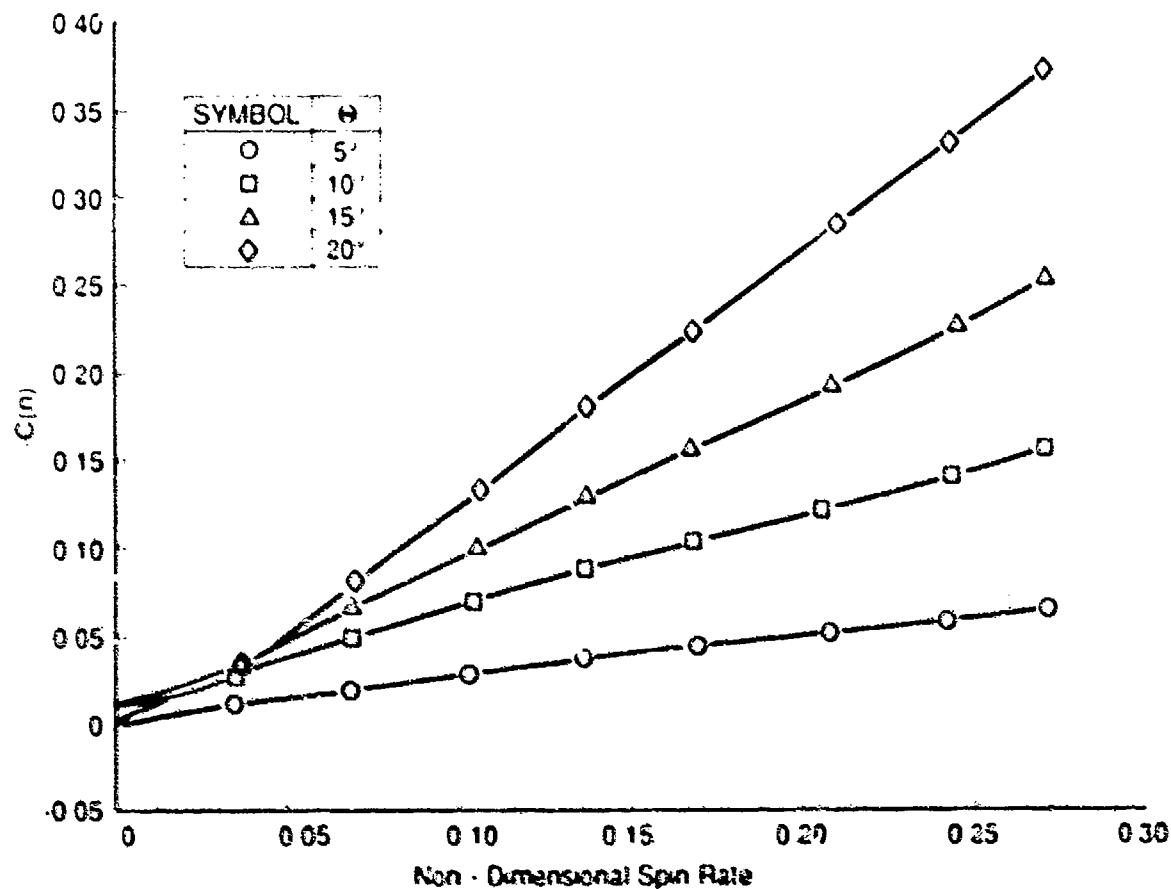


FIGURE 10: EFFECT OF SPIN RATE ON AERODYNAMIC COEFFICIENTS AT MACH NO. = 0.7 AND  $\Theta = 20^\circ$

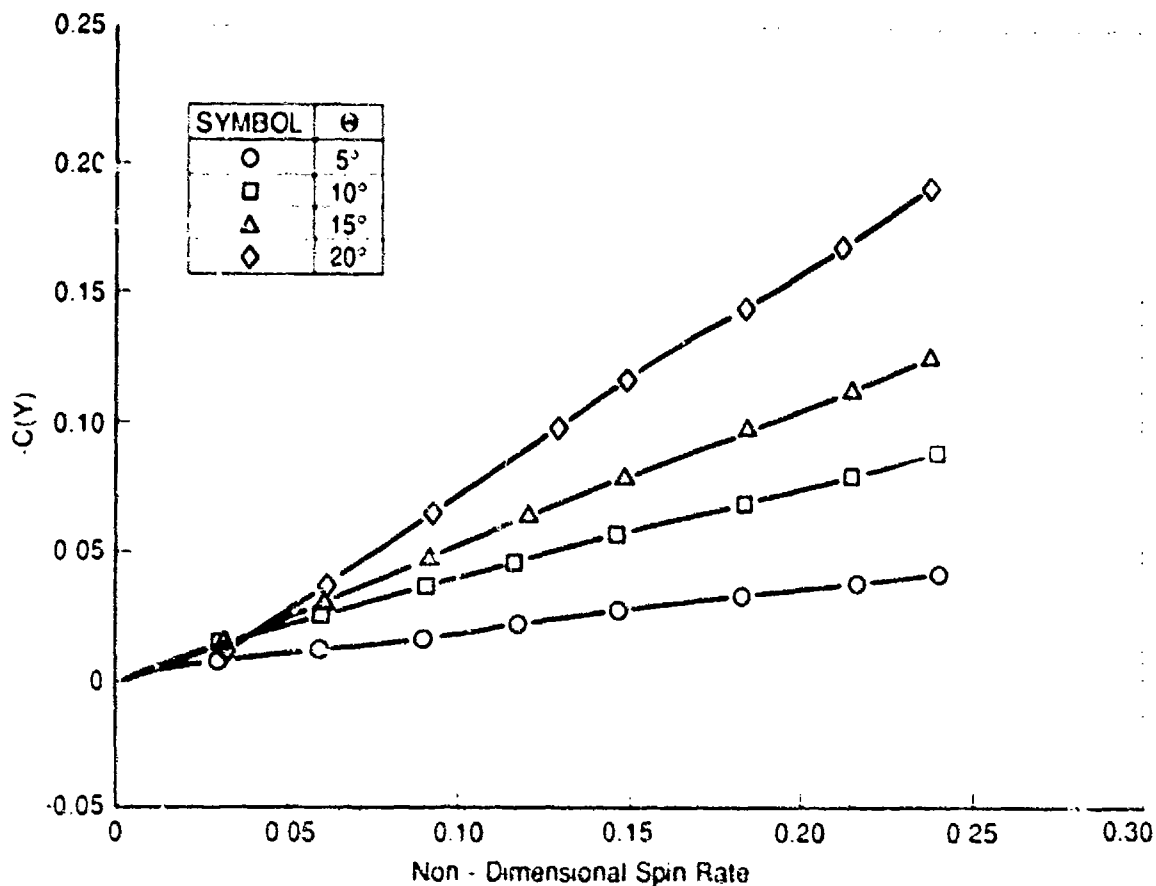


(a)  $C(Y)$  vs Non - Dimensional Spin Rate at Mach No. = 0.7

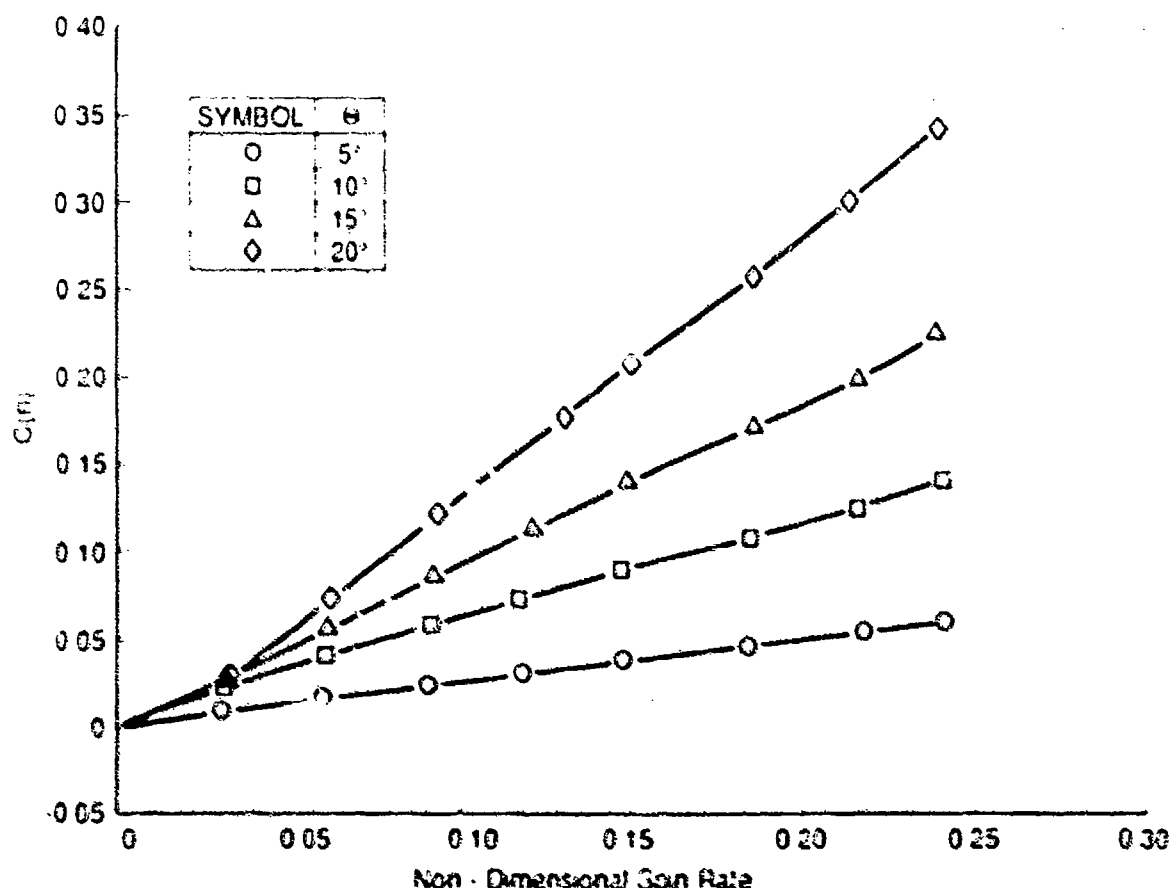


(b)  $C(n)$  vs Non - Dimensional Spin Rate at Mach No. = 0.7

FIGURE 11: SIDE (MAGNUS) FORCE AND YAWING MOMENT COEFFICIENTS vs SPIN RATE

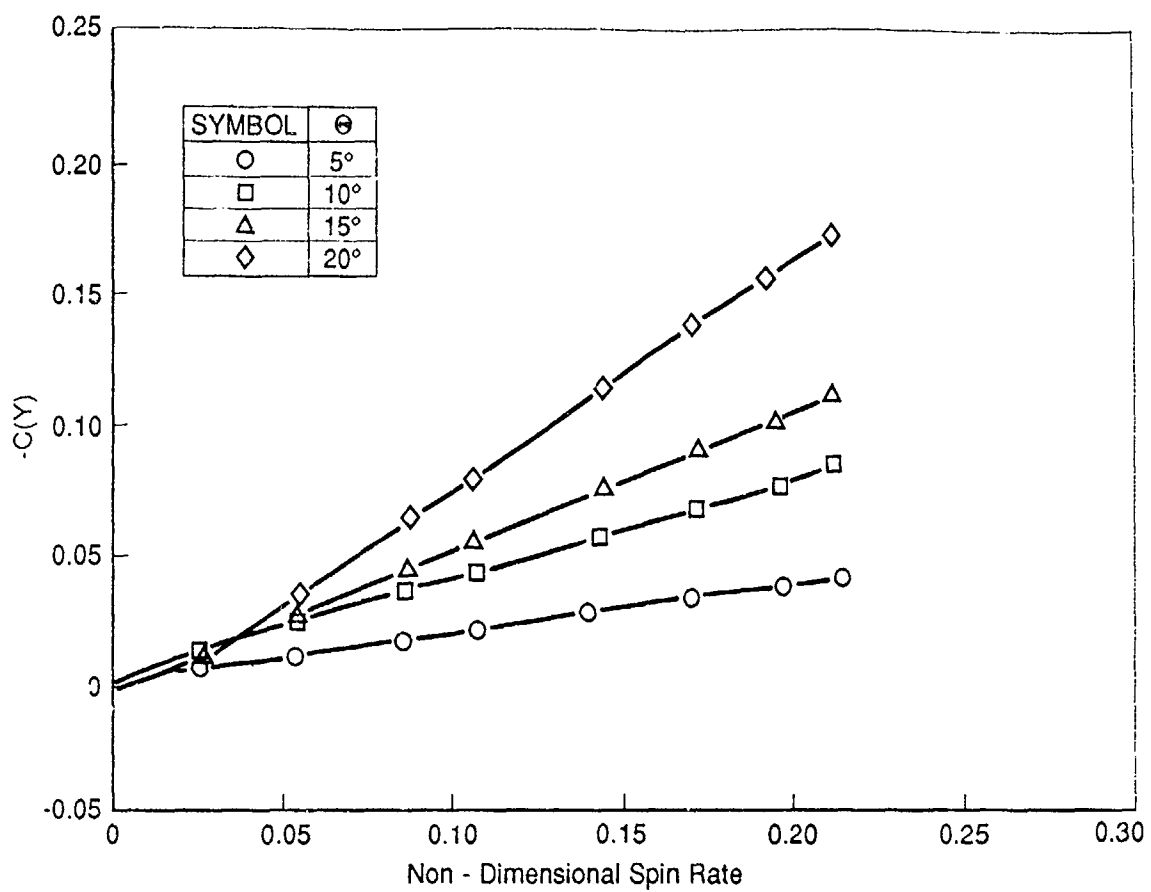


(c)  $C(Y)$  vs Non - Dimensional Spin Rate at Mach No. = 0.8

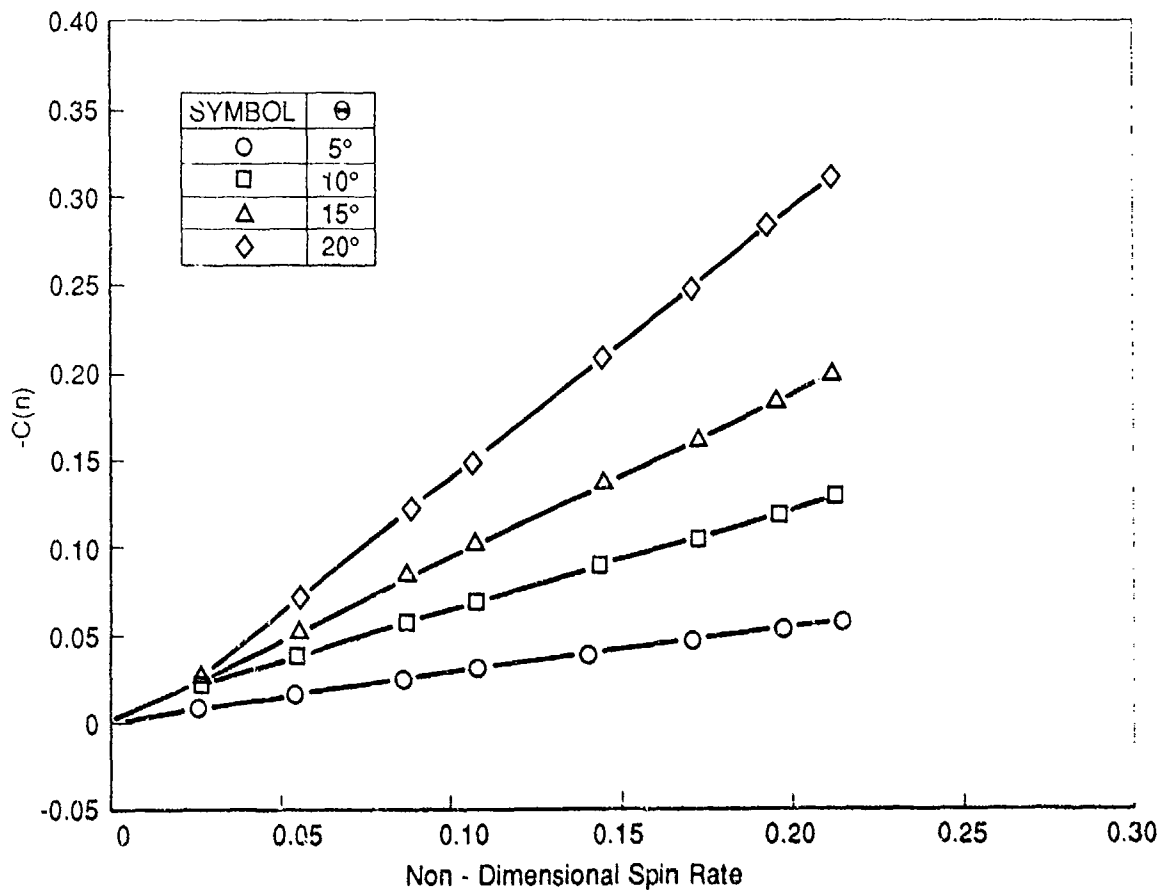


(d)  $C(n)$  vs Non - Dimensional Spin Rate at Mach No. = 0.8

FIGURE 11 (CONT'D) SIDE (MAGNUS) FORCE AND YAWING MOMENT COEFFICIENTS vs SPIN RATE

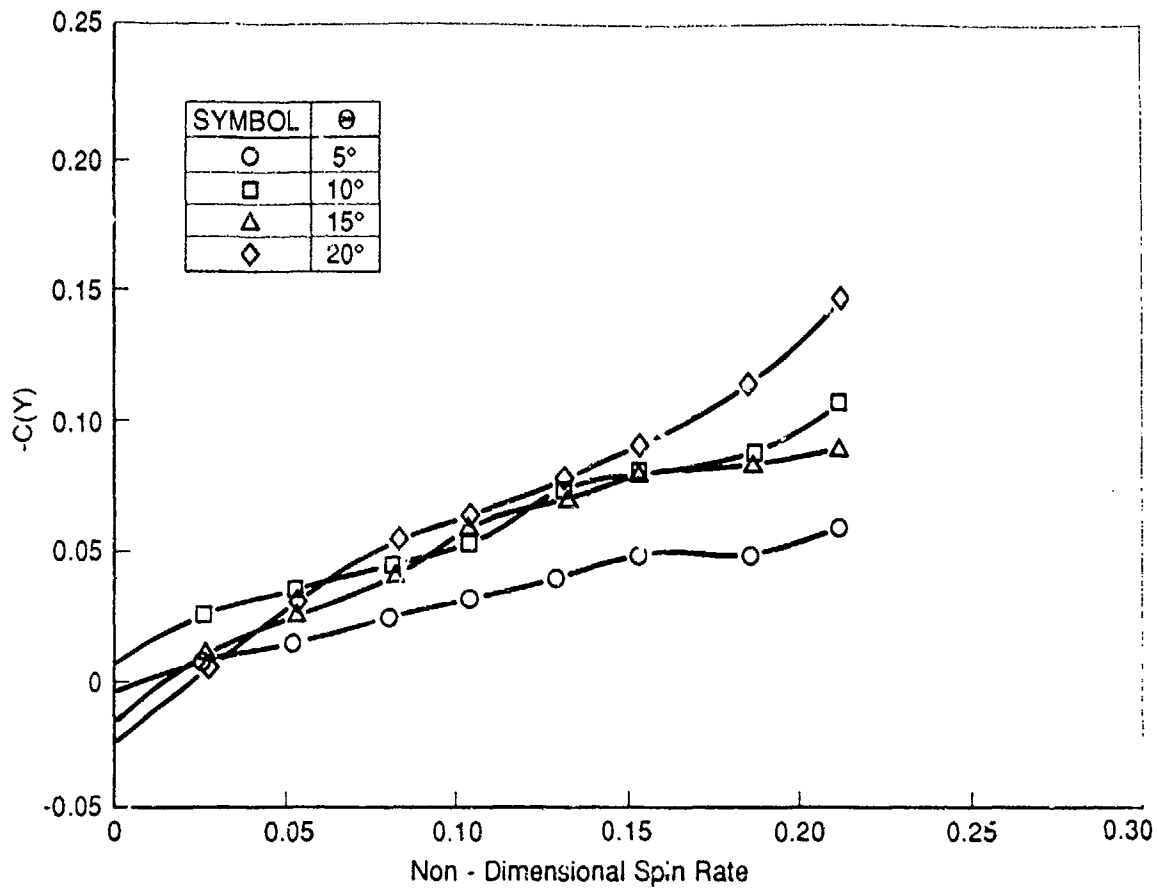


(e)  $C(Y)$  vs Non - Dimensional Spin Rate at Mach No. = 0.9

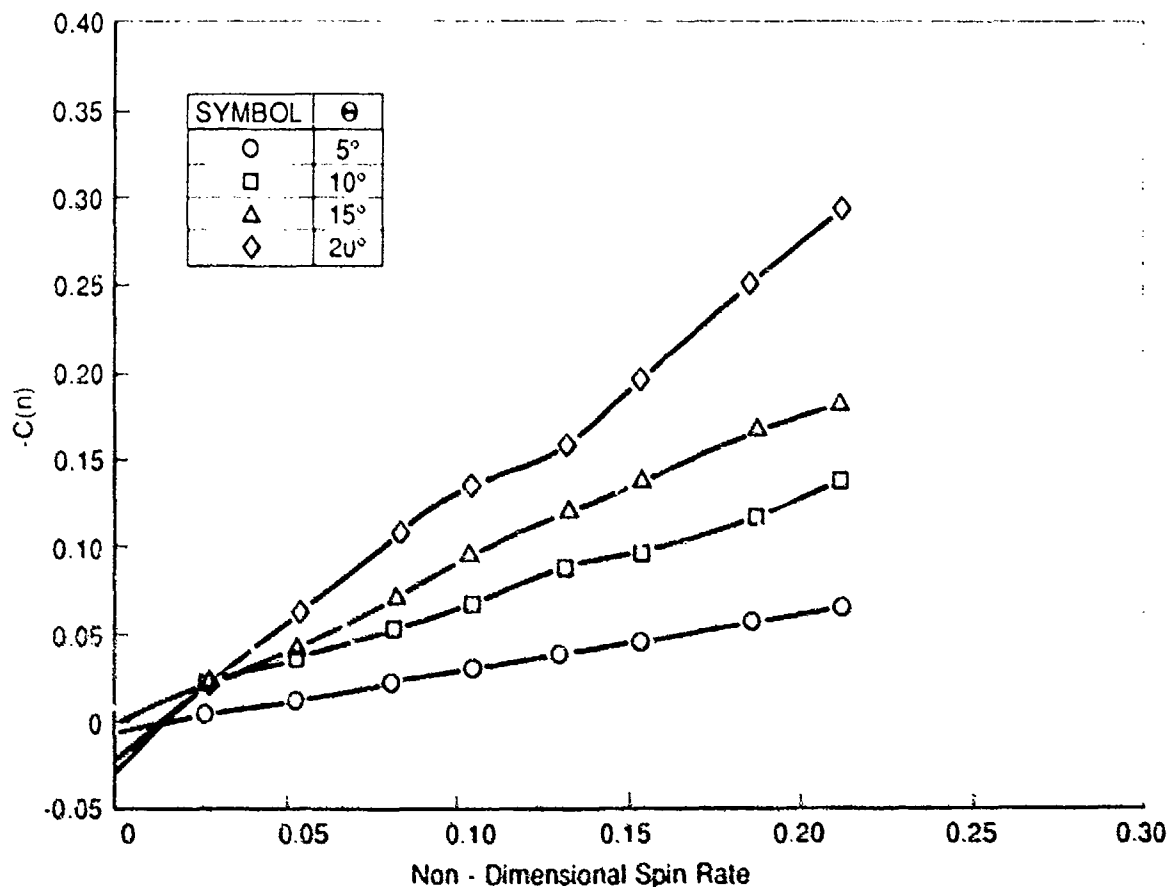


(f)  $C(n)$  vs Non - Dimensional Spin Rate at Mach No. = 0.9

FIGURE 11: (CONT ' D) SIDE (MAGNUS) FORCE AND YAWING MOMENT COEFFICIENTS vs SPIN RATE

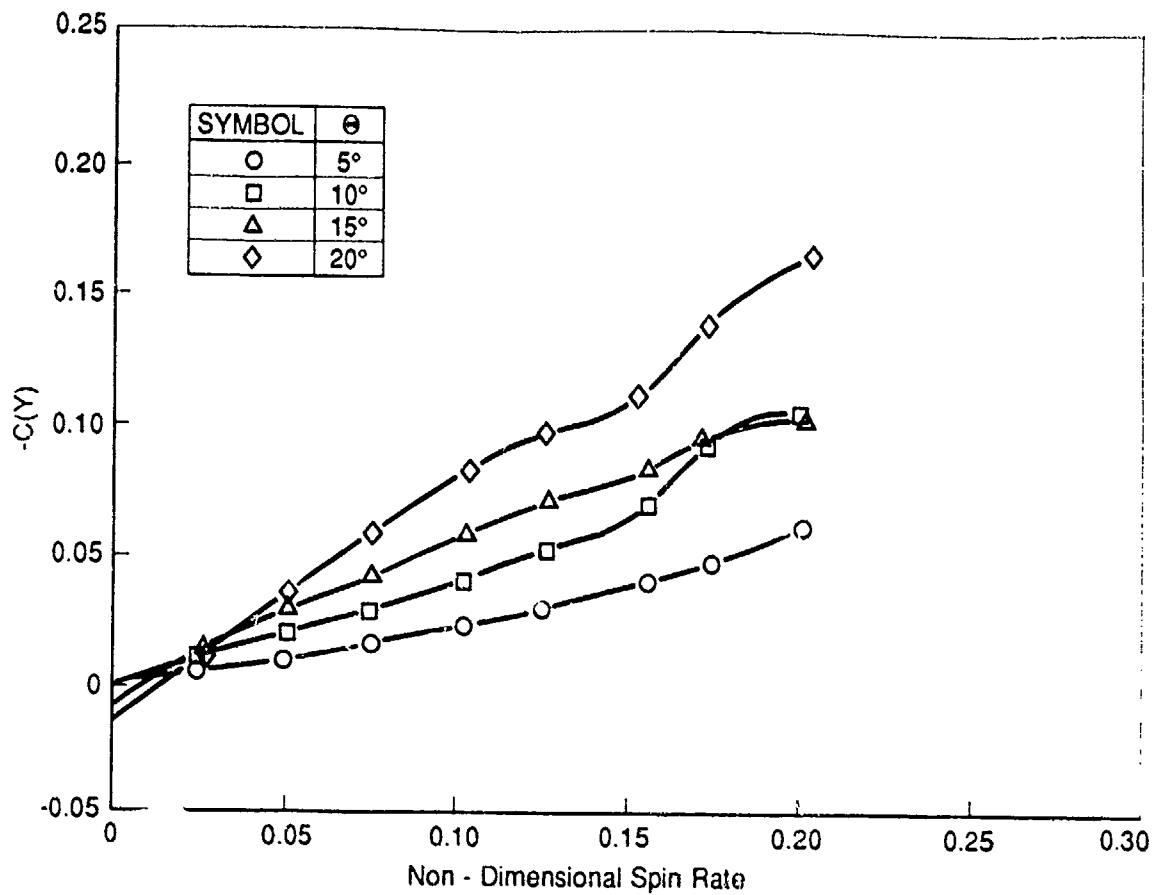


(g)  $C(Y)$  vs Non - Dimensional Spin Rate at Mach No. = 0.95

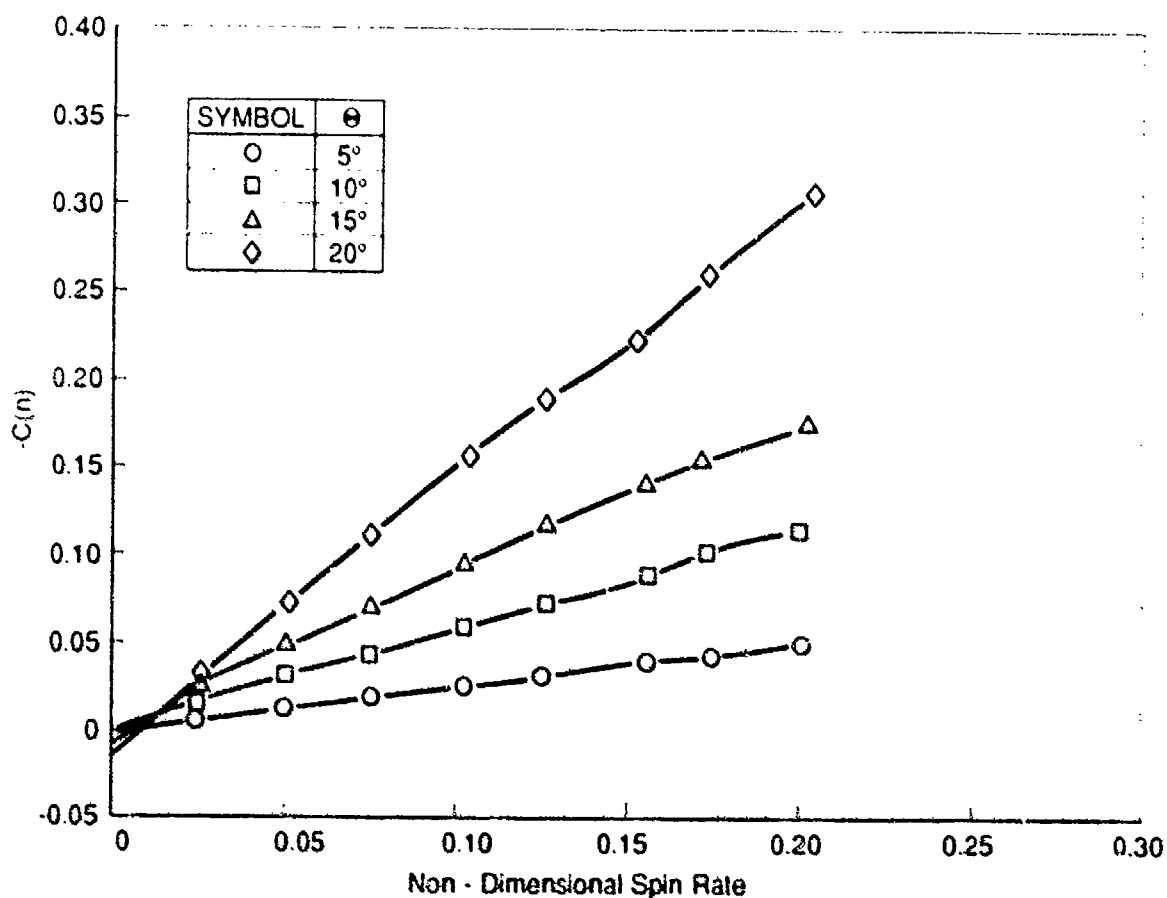


(h)  $C(n)$  vs Non - Dimensional Spin Rate at Mach No. = 0.95

FIGURE 11: (CONT 'D) SIDE (MAGNUS) FORCE AND YAWING MOMENT COEFFICIENTS vs SPIN RATE

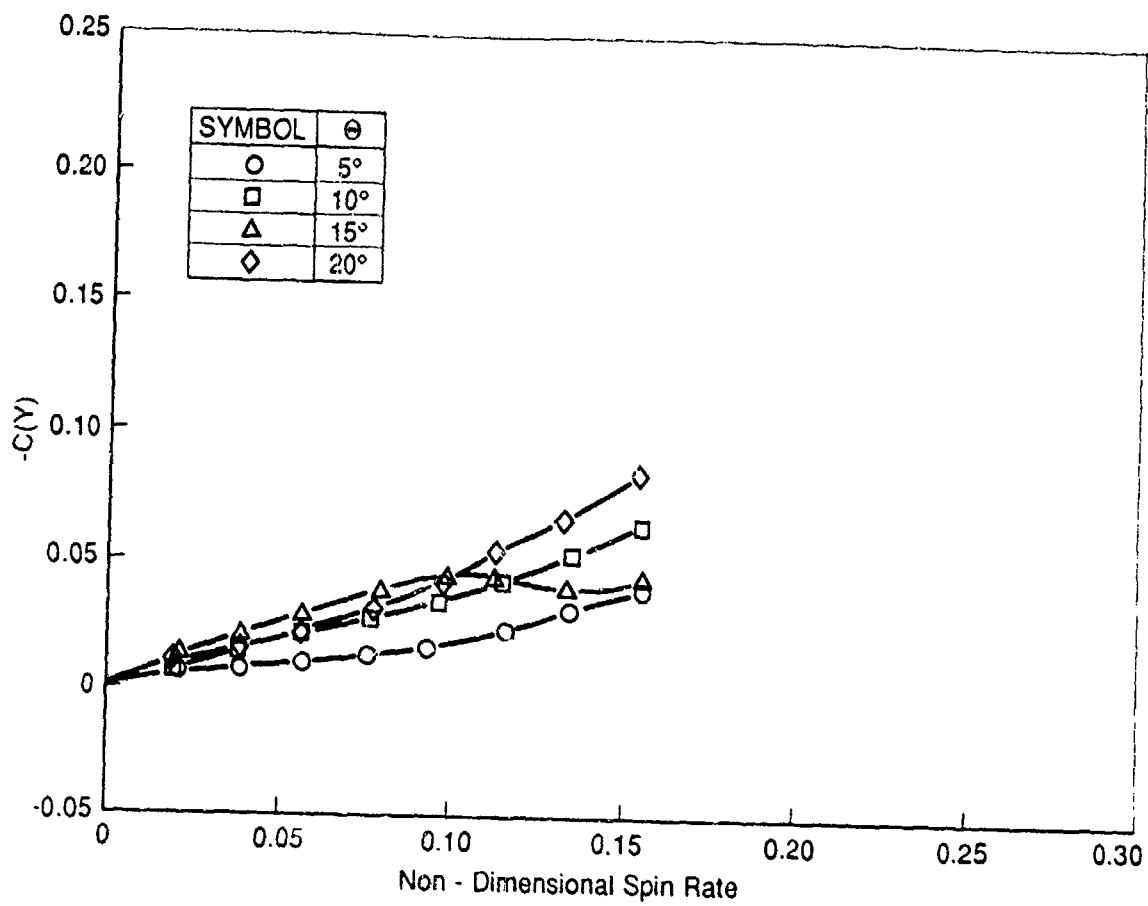


(i)  $C(Y)$  vs Non - Dimensional Spin Rate at Mach No. = 1.0

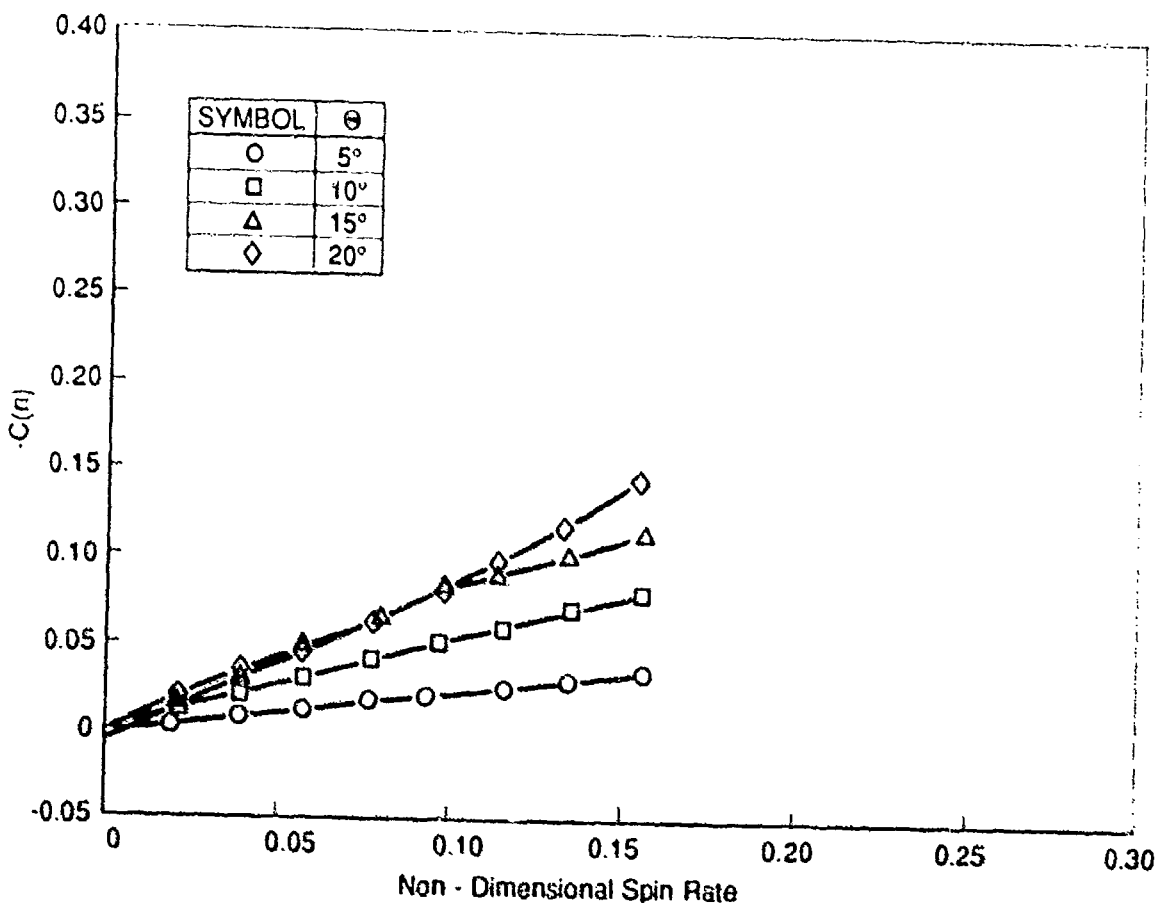


(j)  $C(n)$  vs Non - Dimensional Spin Rate at Mach No. = 1.0

FIGURE 11: (CONT'D) SIDE (MAGNUS) FORCE AND YAWING MOMENT COEFFICIENTS vs SPIN RATE

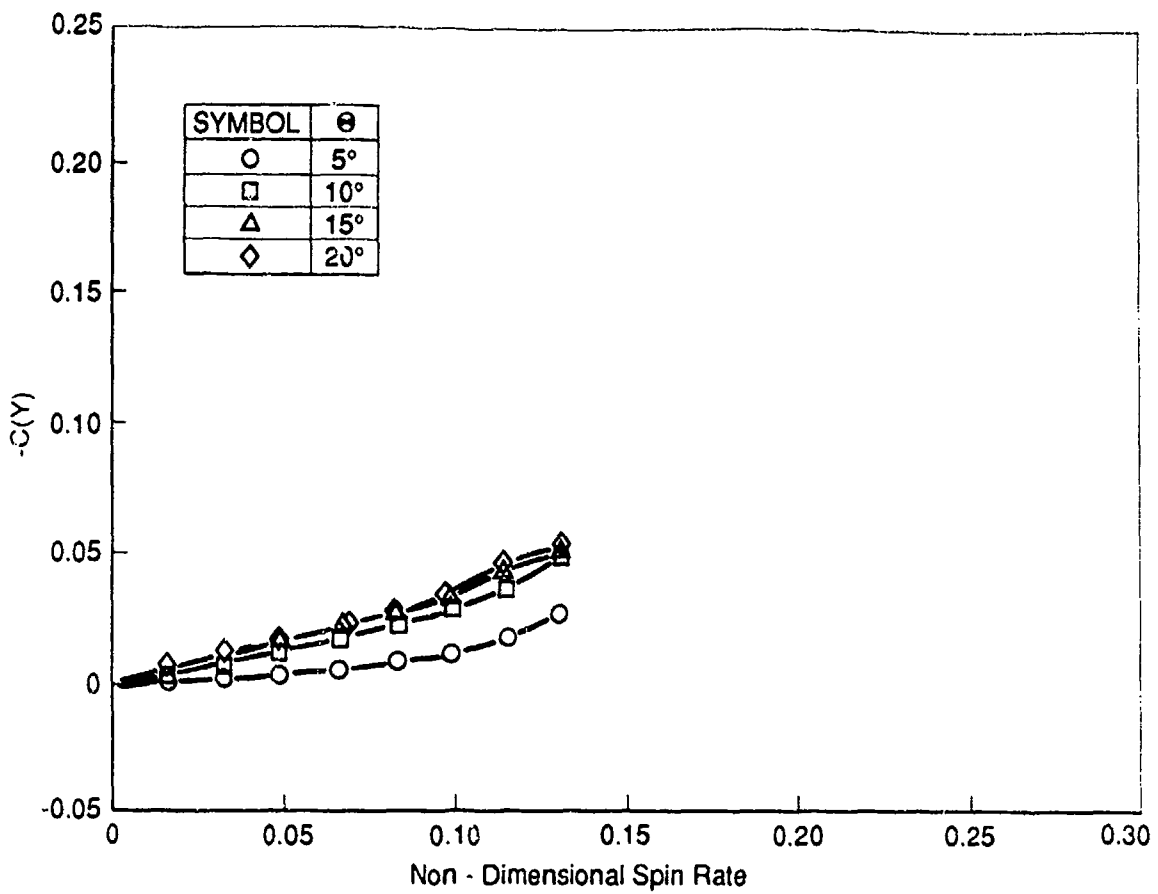


(k)  $C(Y)$  vs Non - Dimensional Spin Rate at Mach No. = 1.4

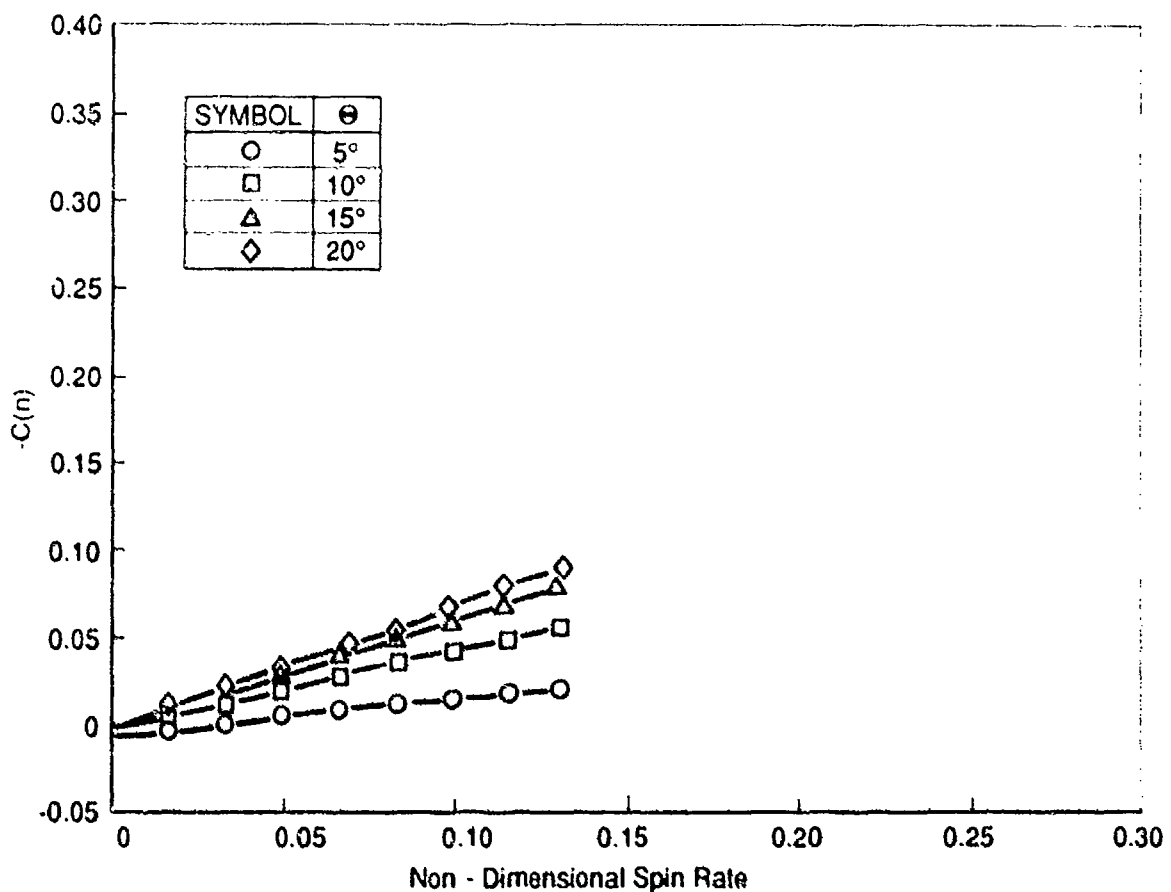


(l)  $C(n)$  vs Non - Dimensional Spin Rate at Mach No. = 1.4

FIGURE 11: (CONT'D) SIDE (MAGNUS) FORCE AND YAWING MOMENT COEFFICIENTS vs SPIN RATE



(m)  $C(Y)$  vs Non - Dimensional Spin Rate at Mach No. = 1.8



(n)  $C(n)$  vs Non - Dimensional Spin Rate at Mach No. = 1.8

FIGURE 11: (CONT'D) SIDE (MAGNUS) FORCE AND YAWING MOMENT COEFFICIENTS vs SPIN RATE

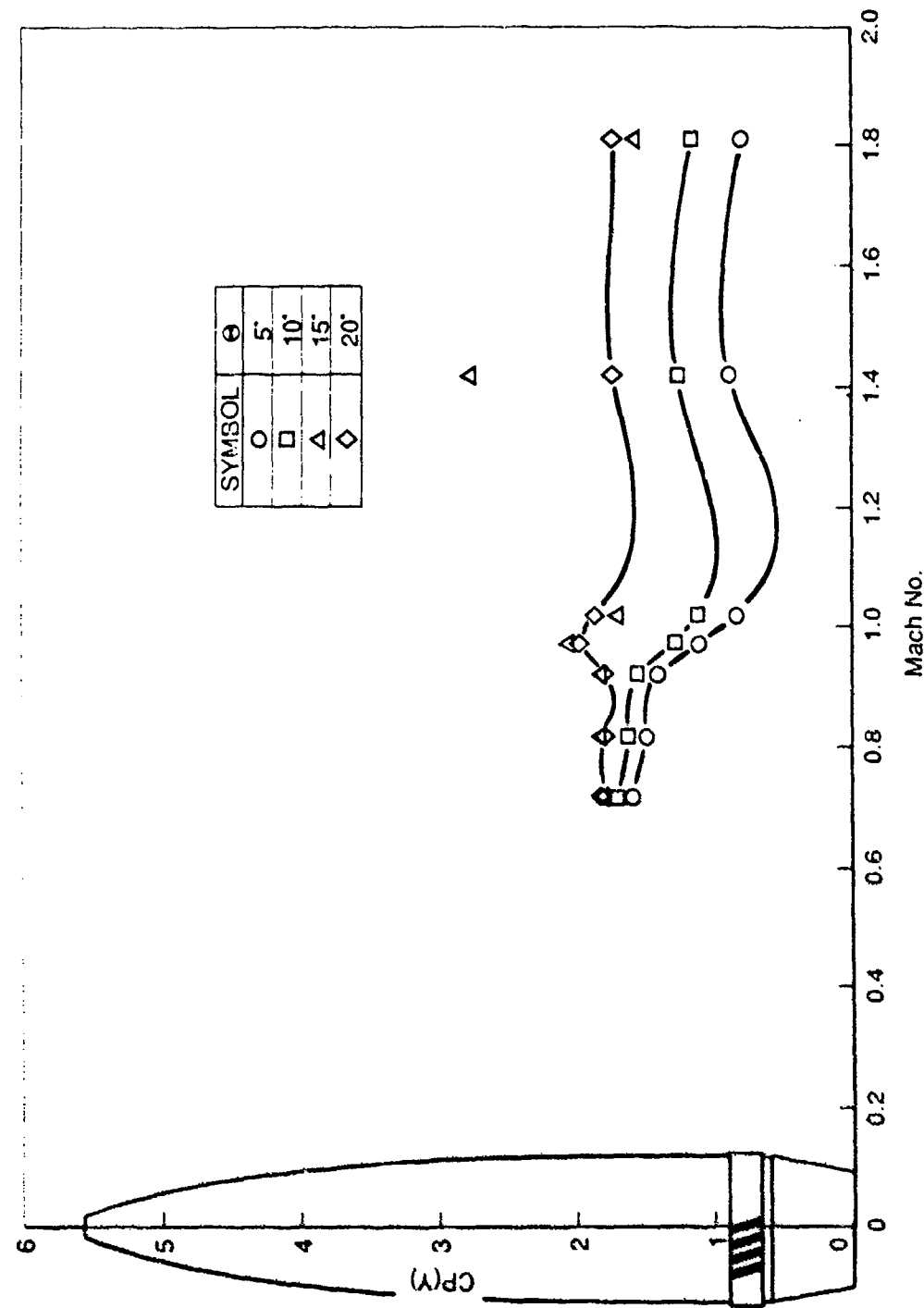


FIGURE 12:  $CP(Y)$  vs MACH NO. AT MAXIMUM SPIN RATE

**DISTRIBUTION**

**AUSTRALIA**

Department of Defence

Defence Central

Chief Defence Scientist  
FAS Science Corporate Management (shared copy)  
FAS Science Policy (shared copy)  
Director, Departmental Publications  
Counsellor, Defence Science, London (Doc Data Sheet Only)  
Counsellor, Defence Science, Washington (Doc Data Sheet Only)  
S.A. to Thailand MRD (Doc Data Sheet Only)  
S.A. to the DRC (Kuala Lumpur) (Doc Data Sheet Only)  
OIC TRS, Defence Central Library  
Document Exchange Centre, DISB (18 copies)  
Joint Intelligence Organisation  
Librarian H Block, Victoria Barracks, Melbourne

Aeronautical Research Laboratory

Director  
Library  
Chief - Flight Mechanics and Propulsion Division  
Head - Flight Mechanics Branch  
Branch File - Flight Mechanics  
Principal Officer, Aerodynamic Research Group  
Principal Officer, Wind Tunnels Research Group  
Authors: D.D. Sivan  
C. Jeremy

Materials Research Laboratory

Director/Library

Defence Science & Technology Organisation - Salisbury  
Library

WSRL

Director  
Chief, Weapons Division  
Head, Weapon Dynamics Group  
Head, Ballistics Group  
Library, Weapons Division  
Maritime Systems Division (Sydney)

Navy Office

Navy Scientific Adviser (3 copies Doc Data sheet)

Army Office

Scientific Adviser - Army (Doc Data sheet only)

Air Force Office

Air Force Scientific Adviser (Doc Data sheet only)

SPARES (10 copies)

TOTAL (50 copies)

## DOCUMENT CONTROL DATA

PAGE CLASSIFICATION

UNCLASSIFIED

PRIVACY MARKING

1a. AR NUMBER AR-006-051	1b. ESTABLISHMENT NUMBER ARL-FLIGHT-MECH-TM-417	2. DOCUMENT DATE AUGUST 1989	3. TASK NUMBER DST 88/035
4. TITLE WIND TUNNEL TESTS OF THE AERODYNAMIC CHARACTERISTICS OF A 155 mm ARTILLERY SHELL		5. SECURITY CLASSIFICATION (PLACE APPROPRIATE CLASSIFICATION IN BOX(S) IE. SECRET (S), CONF. (C) RESTRICTED (R), UNCLASSIFIED (U)).	6. NO. PAGES 30
		<input type="checkbox"/> U <input type="checkbox"/> U <input type="checkbox"/> U	7. NO. REFS. 4
		DOCUMENT      TITLE      ABSTRACT	
8. AUTHOR(S) D.D. SIVAN C. JERMAY		9. DOWNGRADING/DELIMITING INSTRUCTIONS Not applicable.	
10. CORPORATE AUTHOR AND ADDRESS AERONAUTICAL RESEARCH LABORATORY P.O. BOX 4331, MELBOURNE VIC 3001		11. OFFICE/POSITION RESPONSIBLE FOR: SPONSOR _____ DSTO SECURITY _____ - DOWNGRADING _____ - APPROVAL _____ CFPD	
12. SECONDARY DISTRIBUTION (OF THIS DOCUMENT)		Approved for public release.	
OVERSEAS ENQUIRIES OUTSIDE STATED LIMITATIONS SHOULD BE REFERRED THROUGH ASDIS, DEFENCE INFORMATION SERVICES BRANCH, DEPARTMENT OF DEFENCE, CAMPBELL PARK, CANBERRA, ACT 2601			
13a. THIS DOCUMENT MAY BE ANNOUNCED IN CATALOGUES AND AWARENESS SERVICES AVAILABLE TO.... No limitations.			
13b. CITATION FOR OTHER PURPOSES (IE. CASUAL ANNOUNCEMENT) MAY BE		<input checked="" type="checkbox"/> UNRESTRICTED OR <input type="checkbox"/>	AS FOR 13a.
14. DESCRIPTORS Flight control Aerodynamic characteristics Wind tunnel tests		15. DRDA SUBJECT CATEGORIES 0076A 0079A	
16. ABSTRACT The aerodynamic characteristics of a 1/3rd scale 155 mm artillery shell model were measured as a preliminary step in a program to assess the feasibility of using nose mounted controls on a spinning projectile to control its flight path and hence its point of impact. Tests were conducted for Reynolds numbers of 1.0 to 4.0 x 10 <sup>5</sup> , incidences of zero to 20°, Mach numbers of 0.7 to 1.8, and roll rates of zero to 400 rev/s. Results indicate that the use of nose mounted controls to control the attitude and hence the flight path			